Interferometric Measures of Stellar Atmospheres

Interferometric Studies of Single Stars

John Davis

School of Physics

University of Sydney

Why Measure Single Stars?

The measurement of angular diameters leads to the determination of fundamental stellar properties:

- Emergent Fluxes
- Effective Temperatures
- Radii &
- Luminosities

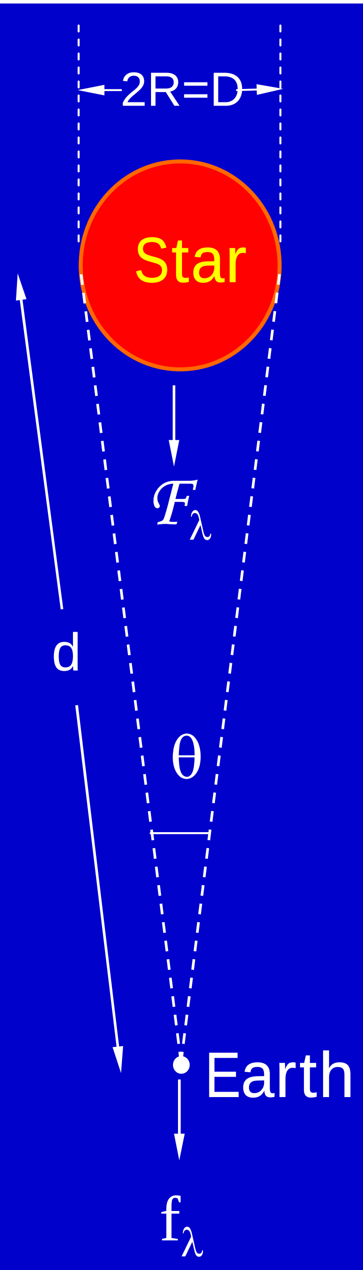

Angular diameter plus flux data:

$$4\pi R^2 \mathcal{F}_\lambda = 4\pi d^2 f_\lambda$$

$$\therefore \qquad \mathcal{F}_\lambda = \frac{4}{\theta^2} . f_\lambda$$

Emergent Flux

$$\int_0^\infty \mathcal{F}_\lambda . d\lambda = \int_0^\infty \frac{4}{\theta^2} . f_\lambda = \sigma T_e^4$$

Effective Temperature

If the distance is known:

$$2R = D = d\,\theta$$

Radius

and $L = 4\pi R^2 \sigma T_e^4$

Luminosity

The Hertzsprung-Russell Diagram

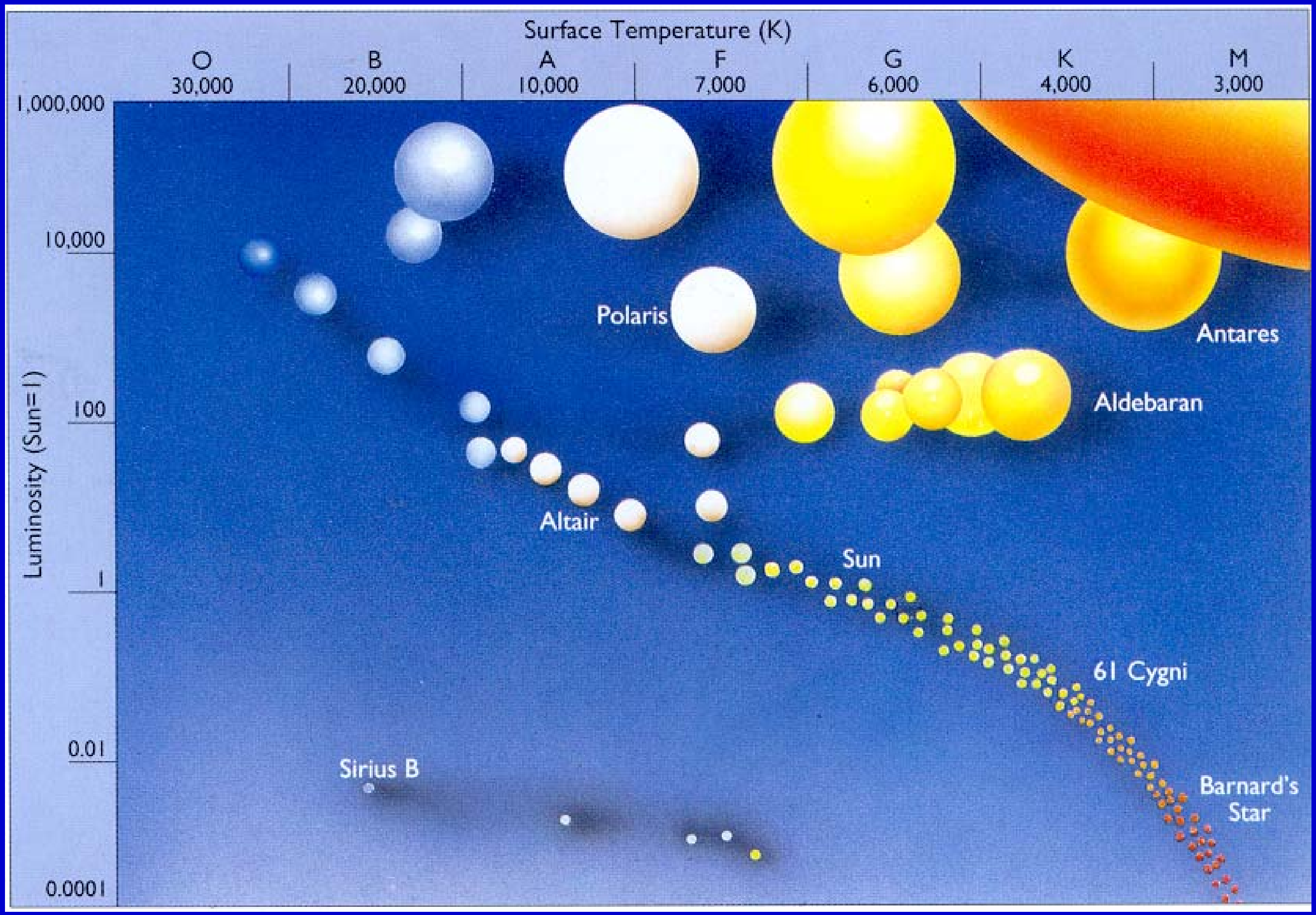

Theoretical HR Diagram and NSII Stars

(Ref: Aufdenberg & Hauschildt, SPIE 4838, 193, 2003)

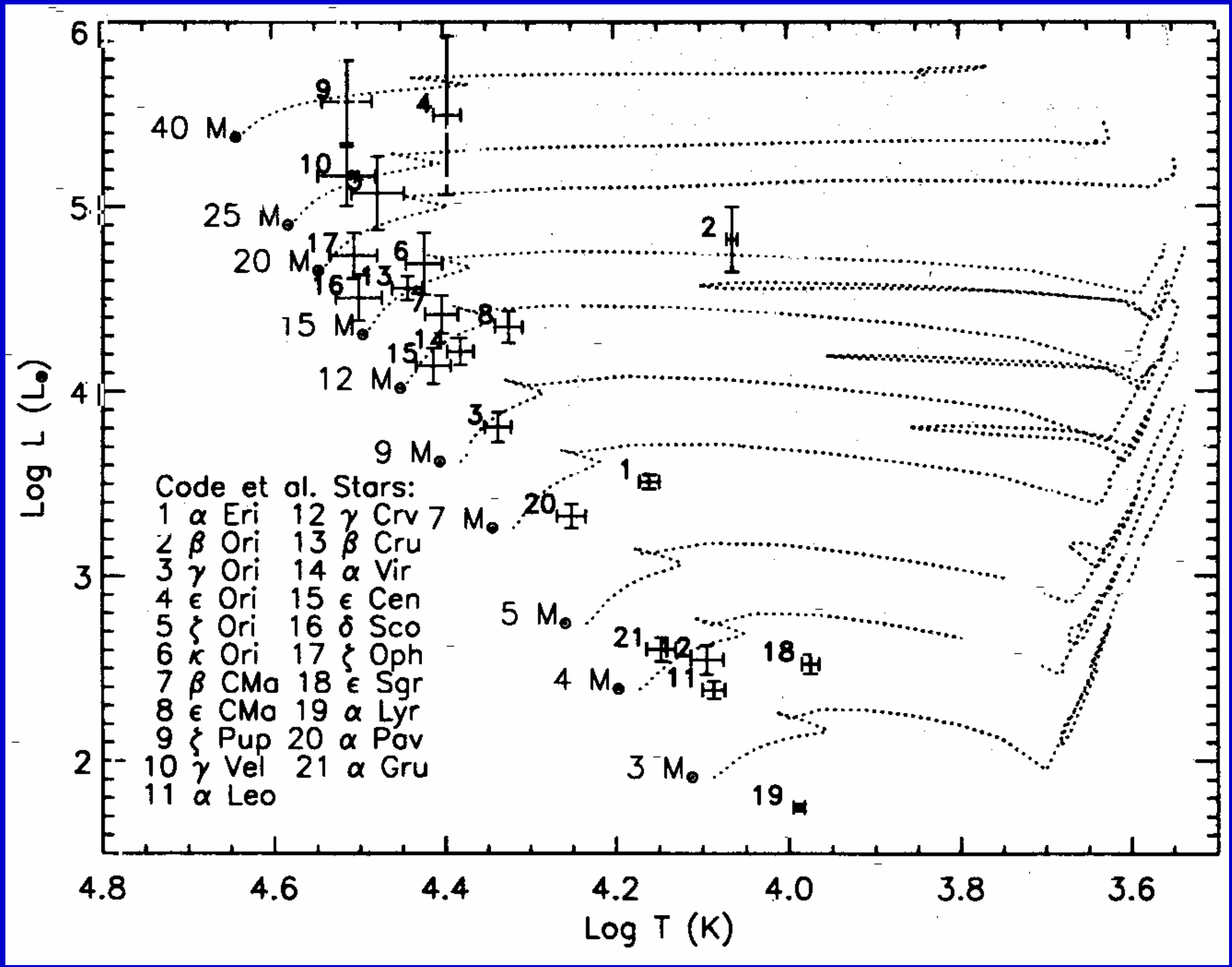

Interferometry and Stellar Atmospheres

Provides tests of model stellar atmosphere predictions either directly or in combination with other data such as spectrophotometry, flux measurements and parallaxes

- Absolute flux distributions
- Effective temperatures
- Limb darkening

A Whole Lot More!

Examples include:

- Rotation – shape
- Pulsating stars – Cepheids and Miras
- Hot star emission envelopes, shells, winds etc.
- Cool star circumstellar dust shells
- Extended corona
- Pre-main sequence objects
- Young stars – structure and morphology
- Novae/Supernovae
- Images – stellar surface features and several of the above items
- etc.

How do we measure the angular diameter of a star ?

Start with a little bit of theory . . . .

(Revision!)

A Little Bit of Theory

The complex visibility V_b and the angular distribution of intensity across a source I_α are a Fourier transform pair:

$$V_b \xleftrightarrow{FT} I_\alpha$$

where $$V_b = |V_b| \exp(i\phi_b)$$

In principle, measurement of $|V_b|$ and ϕ_b over an appropriate range of baseline lengths and orientations (*u*,*v* - plane cover) enable an image/map of the source to be constructed

In Practice . . . .

So far, most interferometric determinations of stellar angular diameters have been made with measurements of $|V_b|^2 = C$ using a single baseline at a time

Calibration by interleaving observations of calibrators: –

$$C_{true}(\text{target}) = C_{obs}(\text{target}) \times \frac{C_{true}(\text{calibrator})}{C_{obs}(\text{calibrator})}$$

These measurements are generally fitted with the relationship for a uniformly illuminated disk:

$$C = |V_b|^2 = |2J_1(x)/x|^2$$

where $x = \pi b \theta_{UD}/\lambda$

Visibility v. Baseline for a Uniformly Illuminated Disk

(Angular Diameter = 2.0 mas: Wavelength = 442 nm)

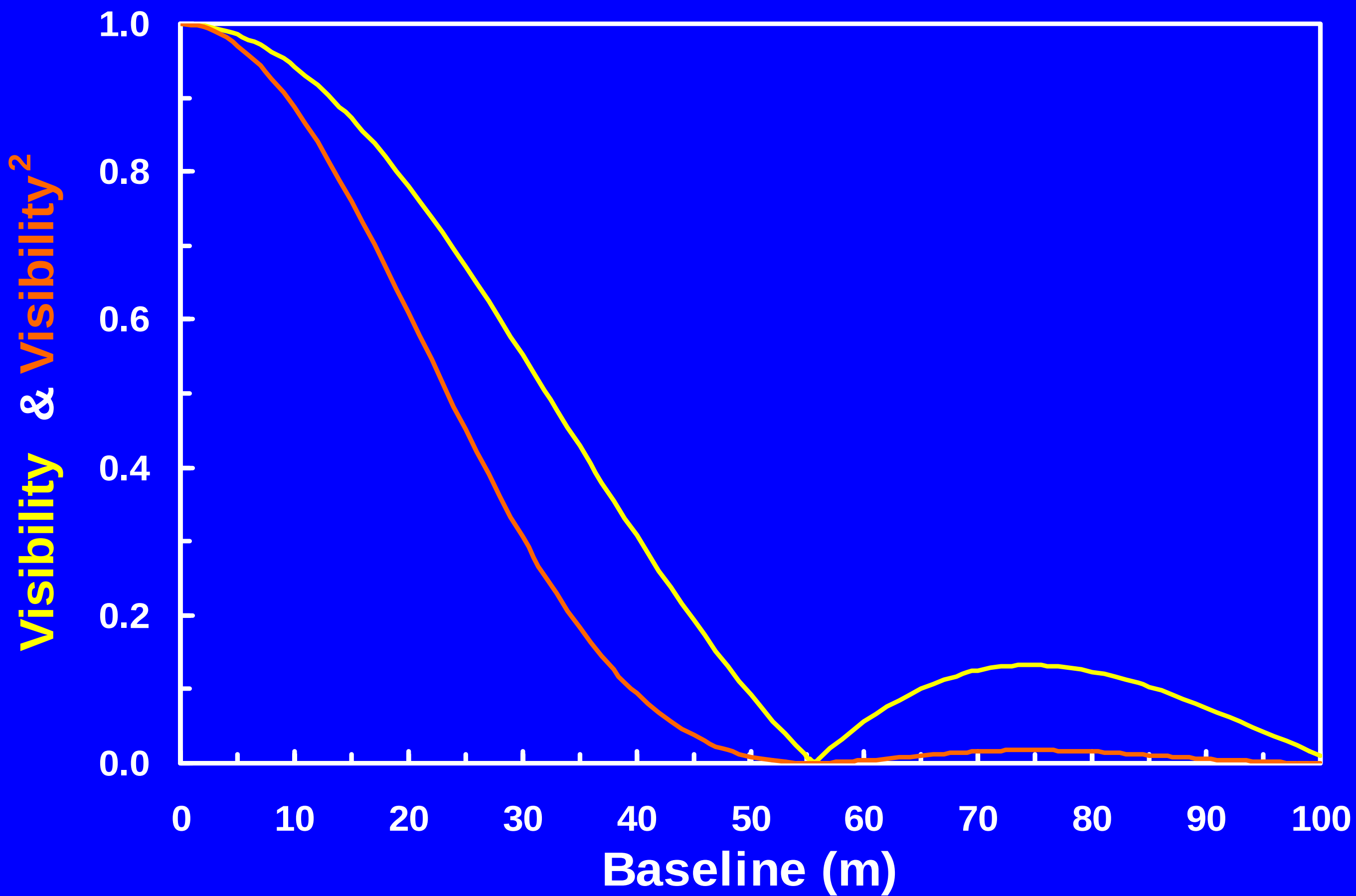

Example Uniform Disk Fit

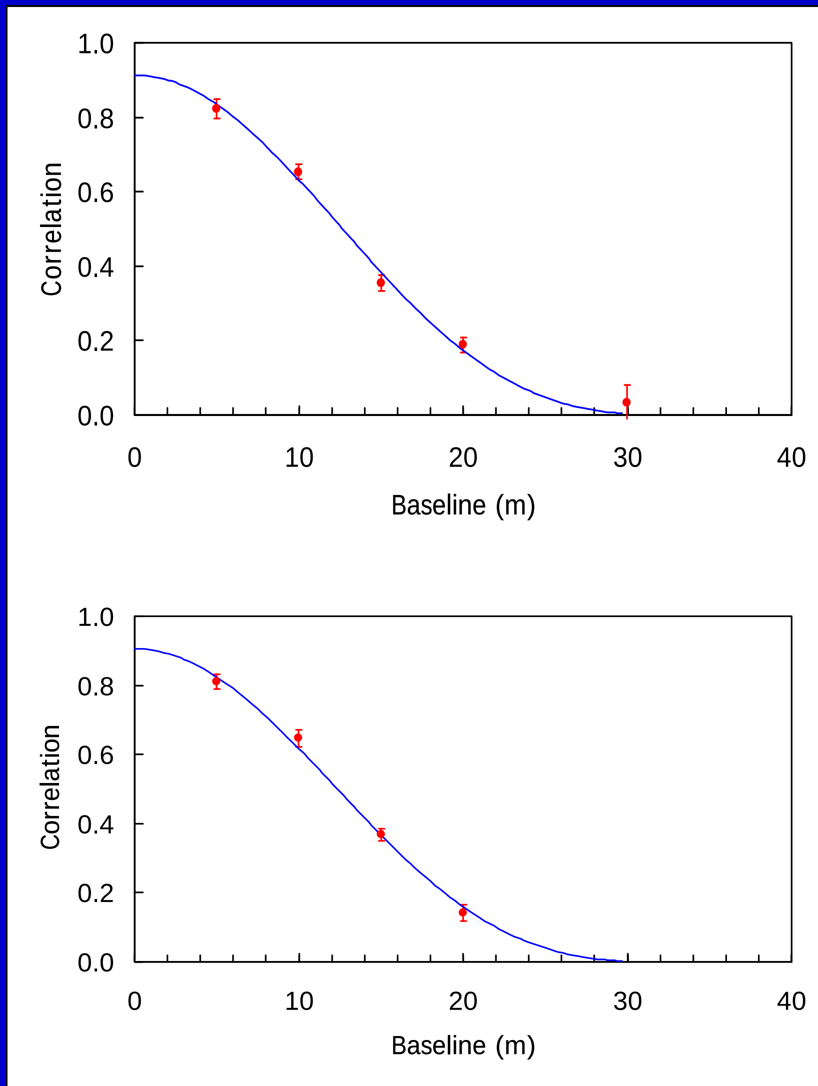

SUSI observations of δ CMa using ε CMa as calibrator

θ_{UD} = 3.474 ± 0.091 mas

SUSI observations of δ CMa using η CMa as calibrator

θ_{UD} = 3.535 ± 0.090 mas

Status of Interferometrically Measured Stellar Angular Diameters

1997

Range in Spectral Type	Luminosity Class				
	I	II	III	IV	V
O	3				1
BO-B4	2	2	3	2	2
B5-B9	2		1	1	1
A0-A3	1			2	5
A5-A7			1		1
F0-F5	3			1	
F6-F8	2				
G0-G5	2	1	2	3	
G6-G9	2	1	12		
K0-K3	3	10	17		
K4-K7	1	1	7		
M0-M4	5	6	18		
M5-M8	1	2	15		
TOTAL:	27	23	76	9	10

Ref: Davis (IAU Symposium 189, 1997)

1999

Range in Spectral Type	Luminosity Class				
	I	II	III	IV	V
O	3				1
BO-B4	2	2	3	2	2
B5-B9	2		1+1	1	1
A0-A3	1			2	5
A5-A7			1		1
F0-F5	4	1		1	
F6-F8	2				
G0-G5	3	1	2	3	
G6-G9	2	1	22		
K0-K3	5	16	31		
K4-K7	3	1	14		
M0-M4	12	13	70		
M5-M8	1	2	31		
TOTAL:	40	37	176	9	10

Evolved Stars	
Carbon	22
M Miras	37
C Miras	5
S Miras	4
TOTAL:	68

Ref: van Belle (Michelson Summer School, 1999)

Status of Interferometrically Measured Stellar Angular Diameters

1997

Range in Spectral Type	Luminosity Class I	II	III	IV	V
O					
BO-B4			1	1	1
B5-B9	1				1
A0-A3				1	3
A5-A7					1
F0-F5	2			1	
F6-F8	2				
G0-G5	2	1		3	
G6-G9	2	1	11		
K0-K3	3	7	11		
K4-K7	1		6		
M0-M4	5	6	15		
M5-M8	1		9		
TOTAL:	19	15	53	6	6

2003

Range in Spectral Type	Luminosity Class I	II	III	IV	V
O					
BO-B4	1		1	1	1
B5-B9	1		1		2
A0-A3				1	3
A5-A7					1
F0-F5	3		1	1	
F6-F8	5				
G0-G5	3	1		3	
G6-G9	1		20	1	
K0-K3	1	9	34	1	1
K4-K7	1		12		
M0-M4	4	5	37		
M5-M8	1	1	15		
TOTAL:	21	16	121	8	8

Restricted to results with $\sigma_\theta < \pm 5\%$

Limb Darkening

Limb-Darkening Correction

- The uniform disk angular diameter is not the true angular diameter and must be adjusted to obtain the true limb-darkened angular diameter
- For compact atmospheres LD and UD transforms are almost identical in shape to first null but differ in scale
- A scaling correction, derived from a model atmosphere CLV, is applied to θ_{UD} to obtain θ_{LD}
- Corrections are generally <10%, depending on T_e, log g and λ, with $\theta_{LD} > \theta_{UD}$

Comparison of Uniform and Limb-Darkened Disk Responses

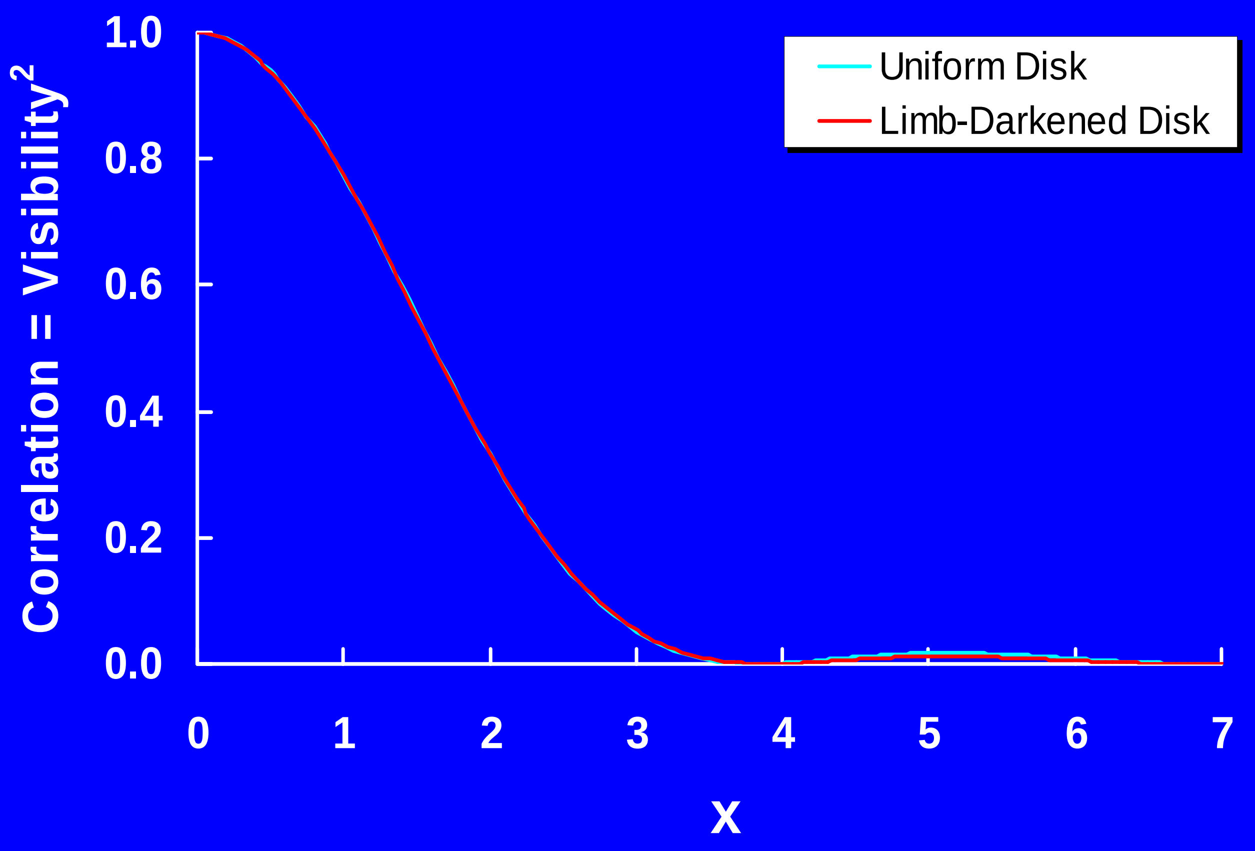

Curves matched at correlation = 0.3 (θ_{LD}/θ_{UD} = 1.055)

Comparison of Uniform and Limb-Darkened Disk Responses

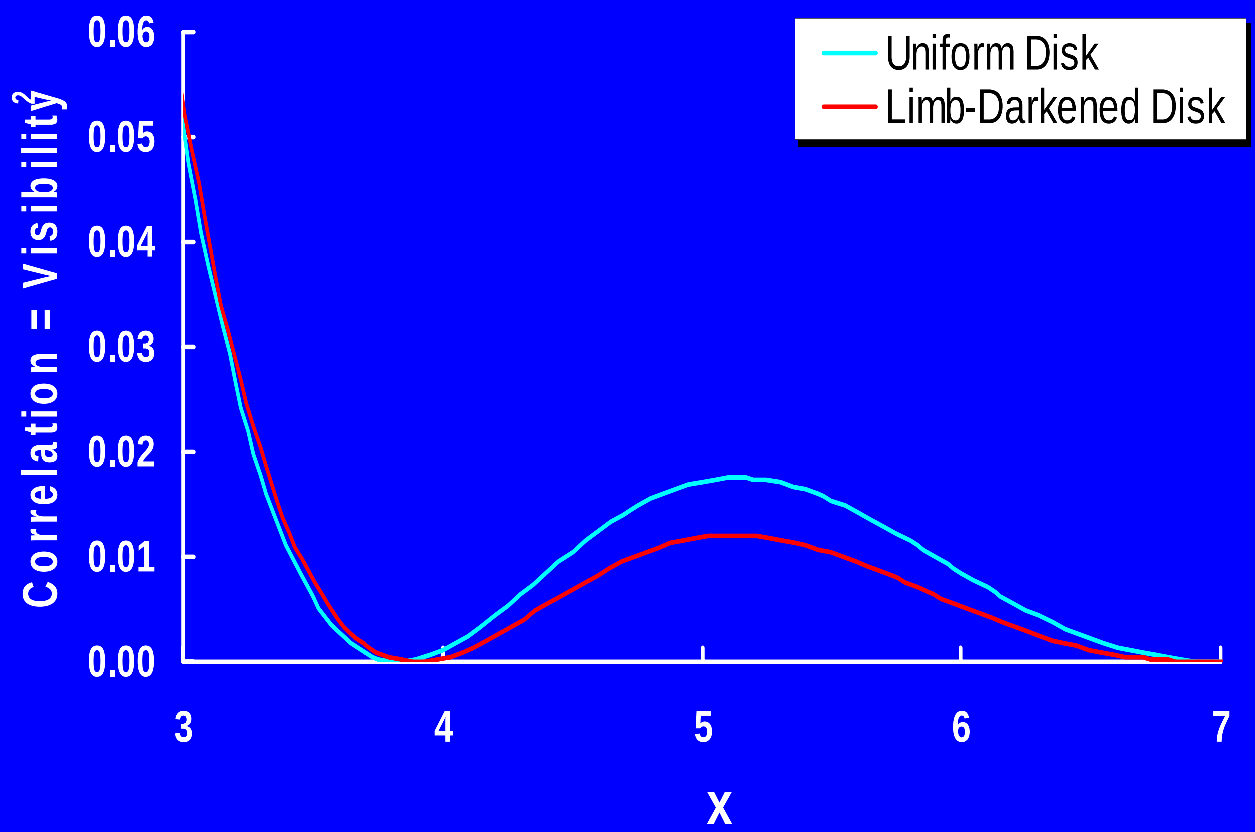

Curves matched at correlation = 0.3 (θ_{LD}/θ_{UD} = 1.055)

Limb Darkening – Centre-to-Limb Intensity Variation

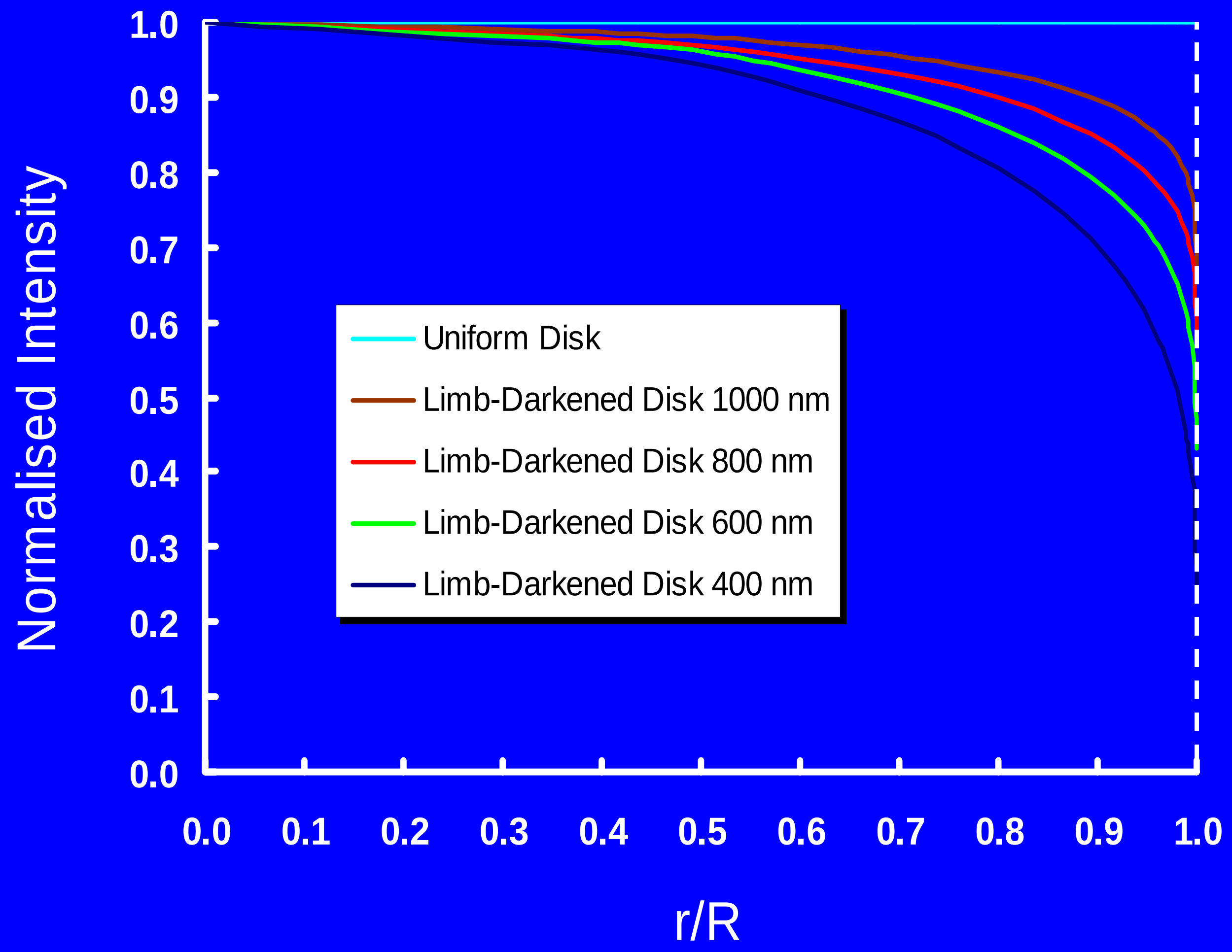

Kurucz model atmosphere for T_e = 10,000 K and log g = 4.0

Limb Darkening – Interferometer Response

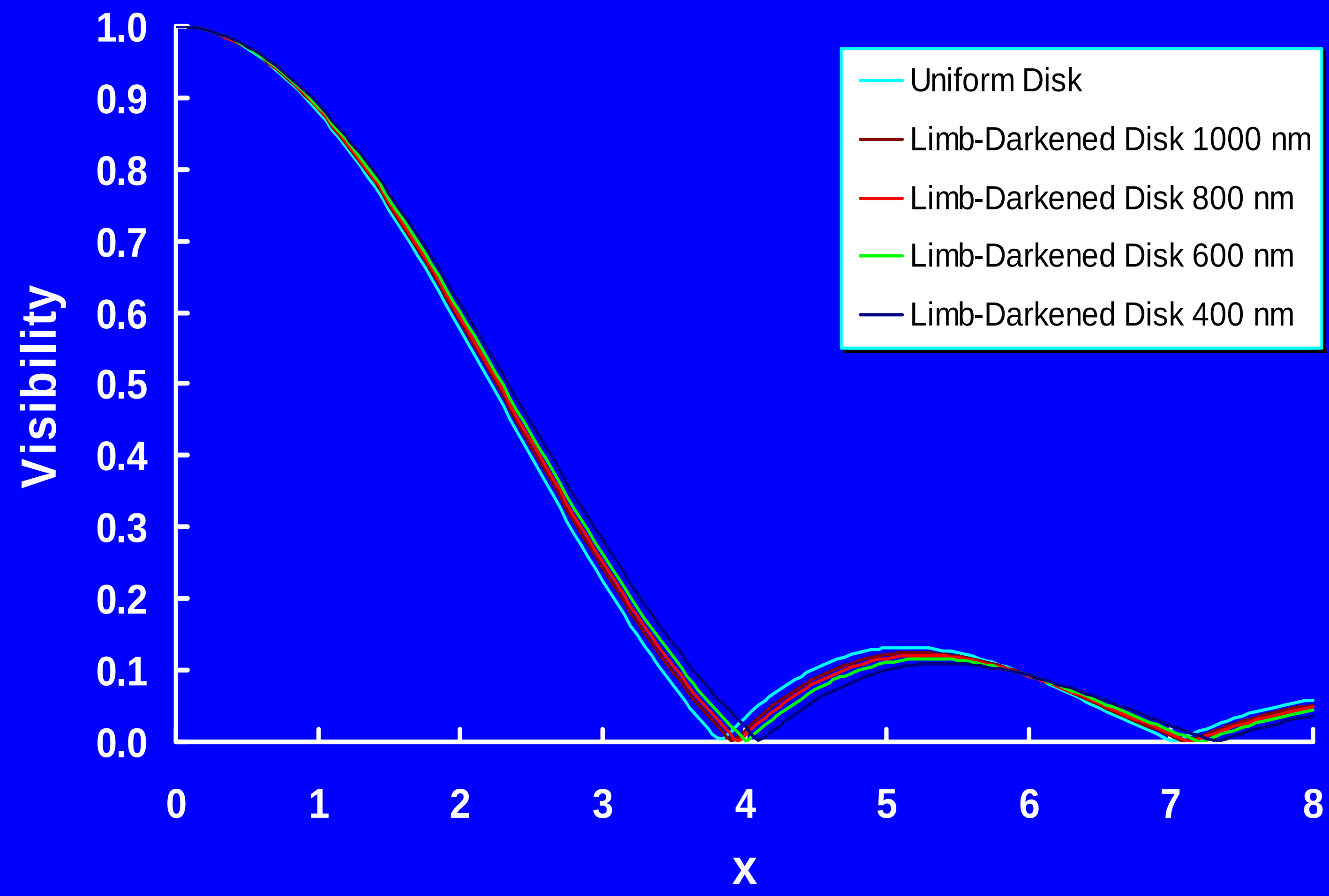

Kurucz model atmosphere for Te = 10,000 K and log g = 4.0

Limb Darkening – Interferometer Response

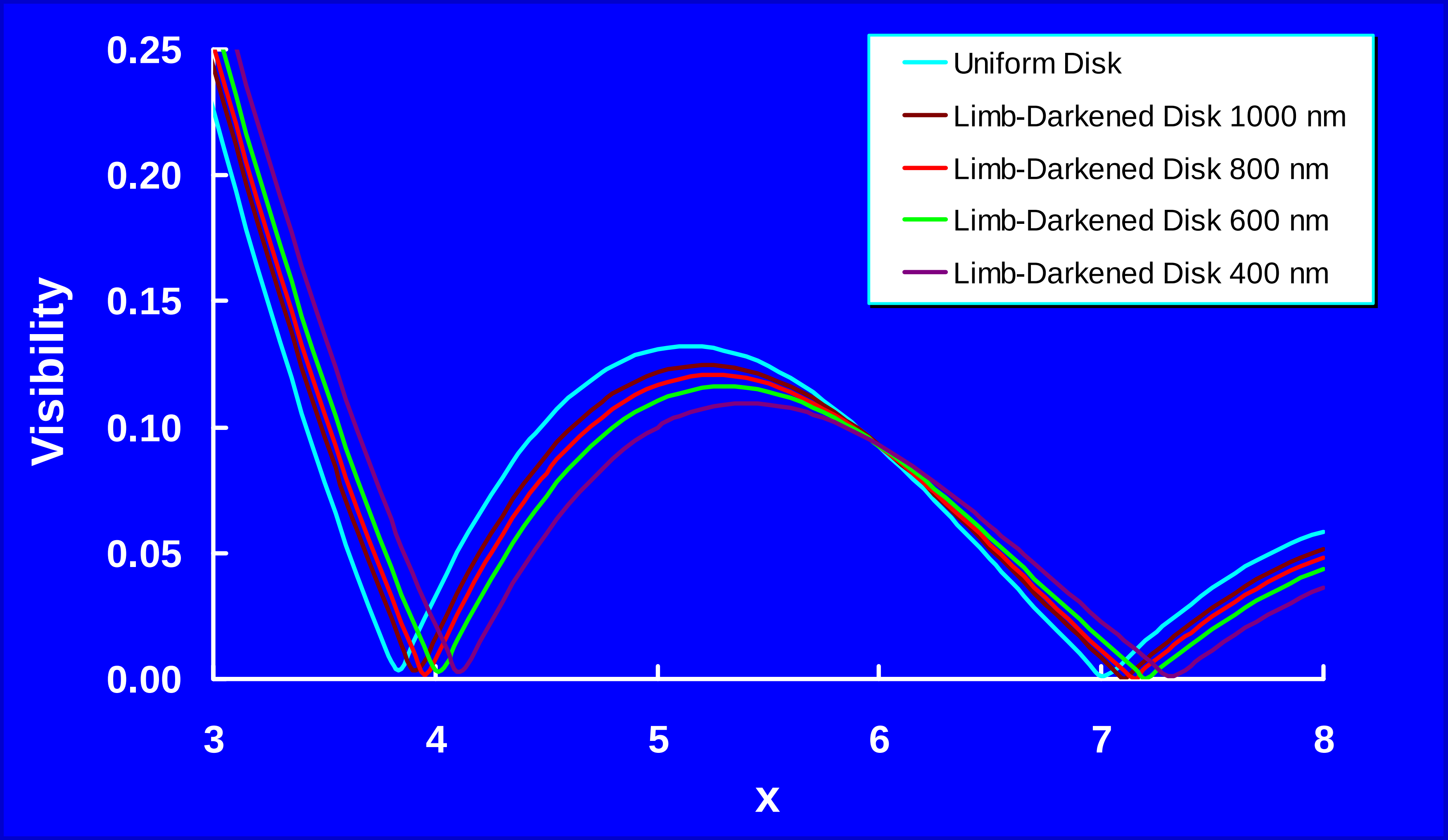

Kurucz model atmosphere for Te = 10,000 K and log g = 4.0

$\rho_\theta = \theta_{LD}/\theta_{UD}$ for Kurucz Model Stellar Atmospheres

(Ref: Davis, Tango & Booth, MNRAS, 318, 387, 2000)

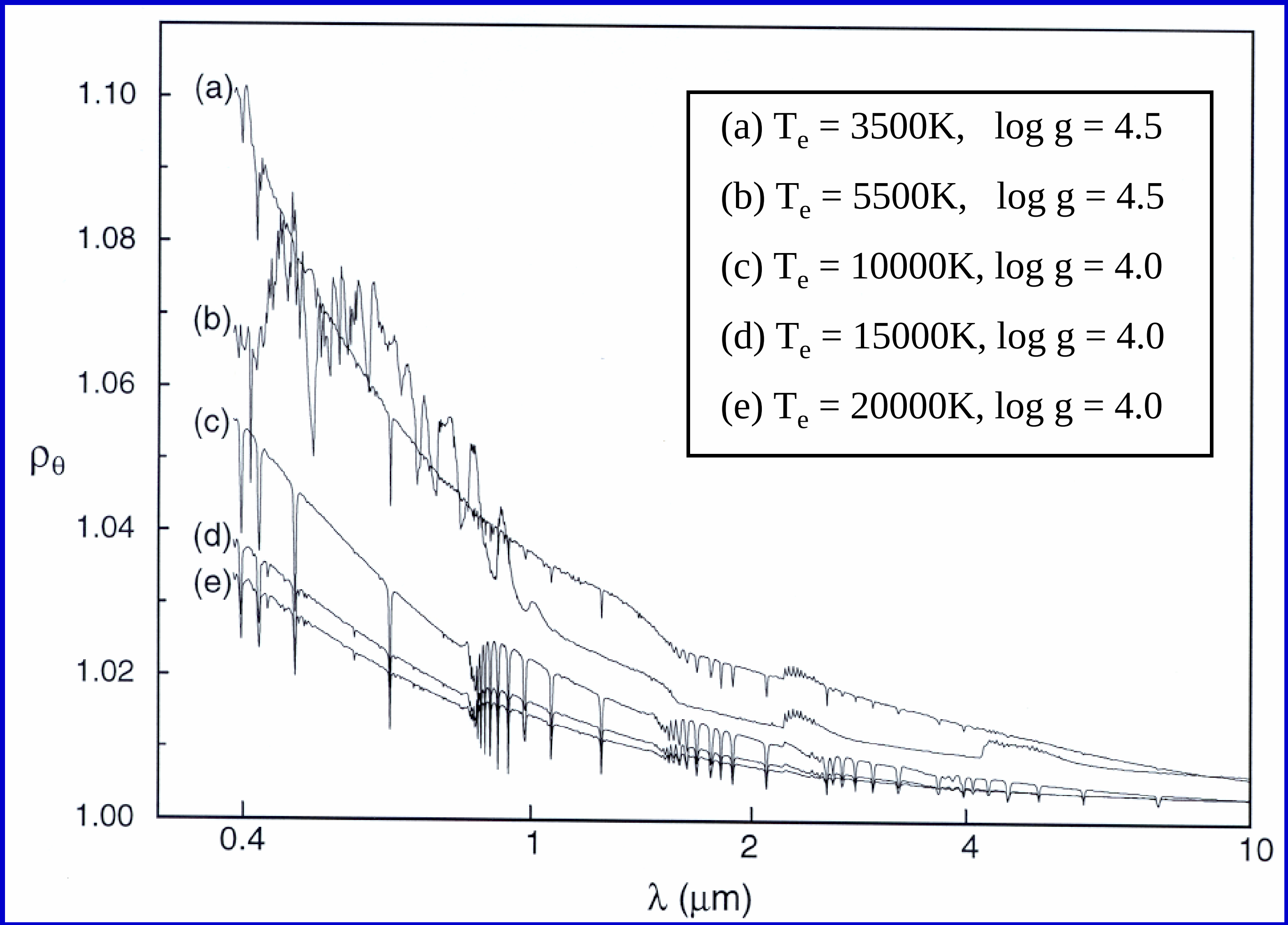

Limb Darkening for M-type Mira Models

(Ref: Hofmann, Scholz & Wood, A&A, 339, 846, 1998)

Centre-to-Limb Intensity Variation

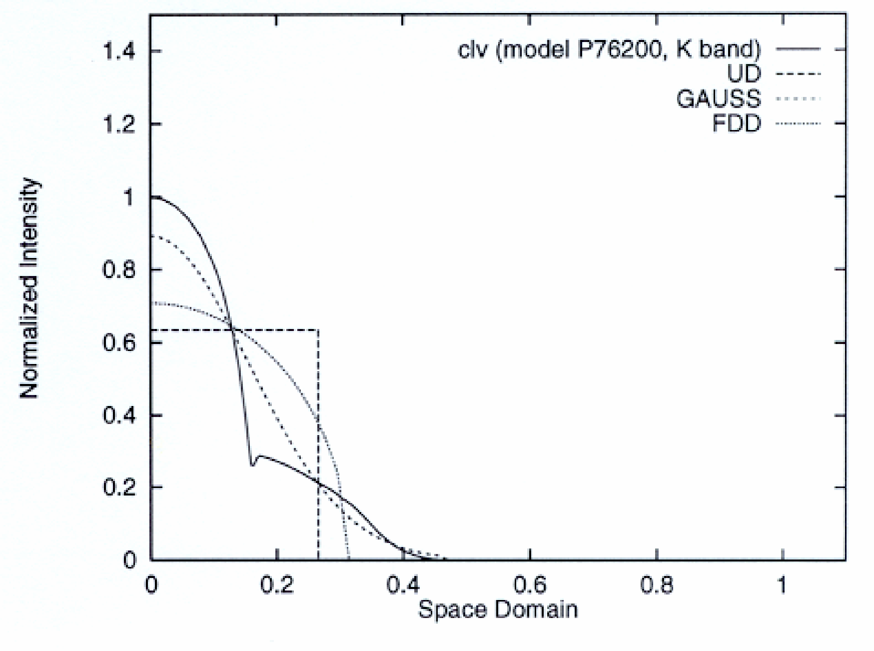

Interferometer Response

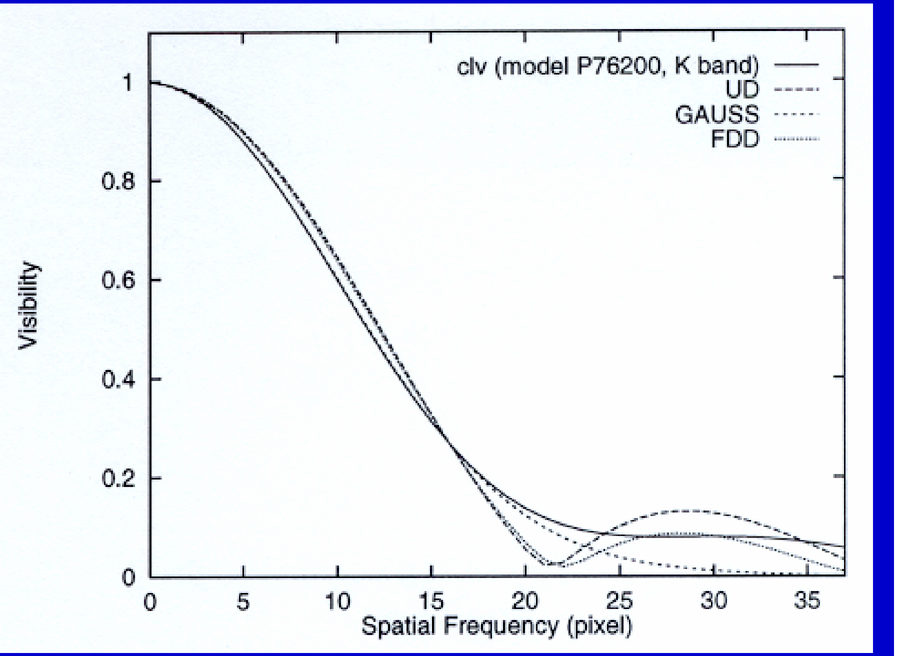

Observations of Mira W Hya

(Ref: Haniff, Scholz & Tuthill, MNRAS, 276, 640, 1995)

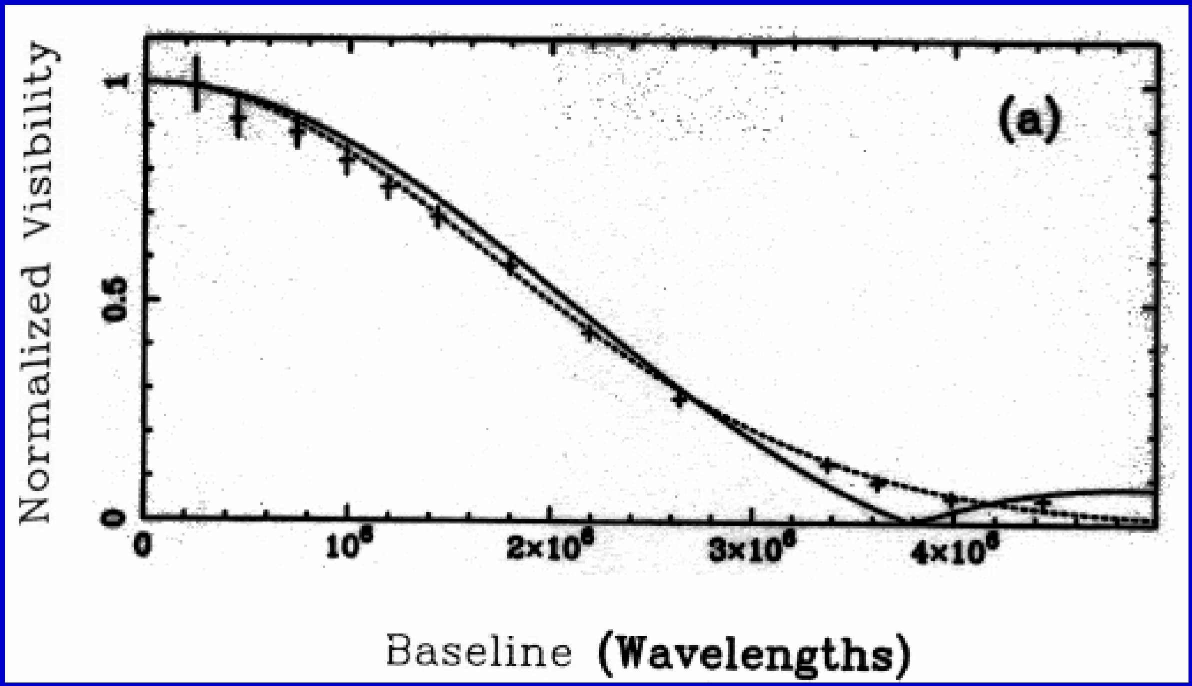

——— Model fit ----- Gaussian fit

Measuring Limb Darkening

Obviously difficult because of the need to measure the low fringe visibilities beyond the first null

Two approaches:

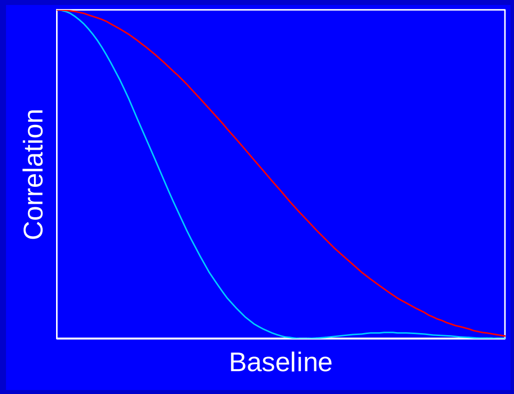

1. Wavelength bootstrapping – fringe-track at a long wavelength while recording measurements at shorter wavelengths

2. Phase or baseline bootstrapping – with an array of three or more elements fringe track on the short baselines while measuring the fringe visibility on all baselines

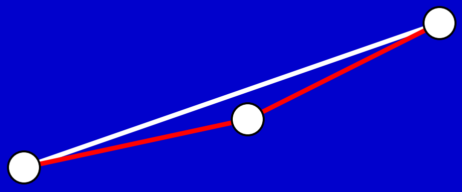

Limb Darkening for Arcturus

(Ref: Quirrenbach et al., A&A, 312, 160, 1996)

α Bootis   550 nm

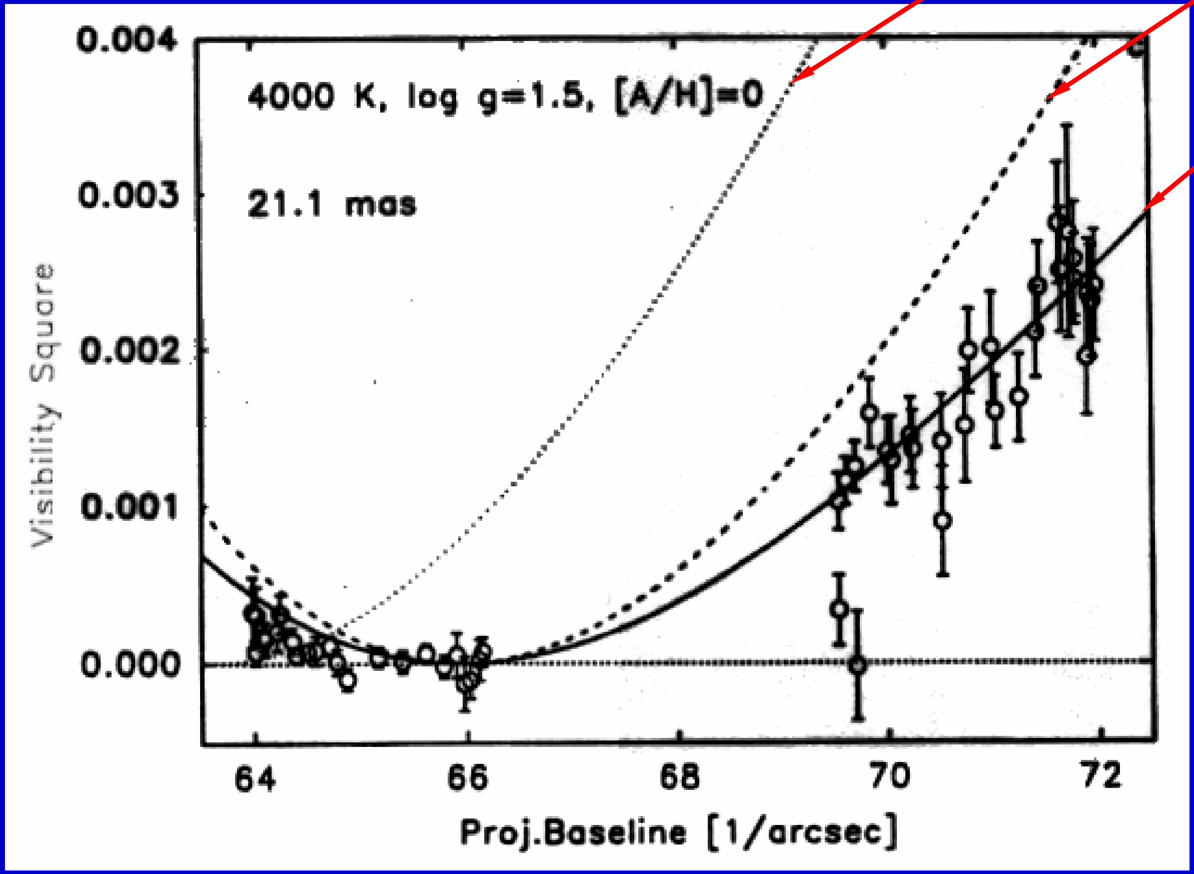

θ_{UD} = 19.18 mas: best fit at short baselines

θ_{UD} = 18.50 mas: null matched to model

Model (Manduca et al., A&A, 61, 809, 1977)

Mark III data

Limb Darkening by Phase Bootstrapping

Pioneered at NPOI

(Ref: Armstrong et al., ASP 154, CD-1931, 1998)

See also:

Hajian et al., ApJ, 496, 484, 1998

Wittkowski et al., A&A, 377, 981, 2001

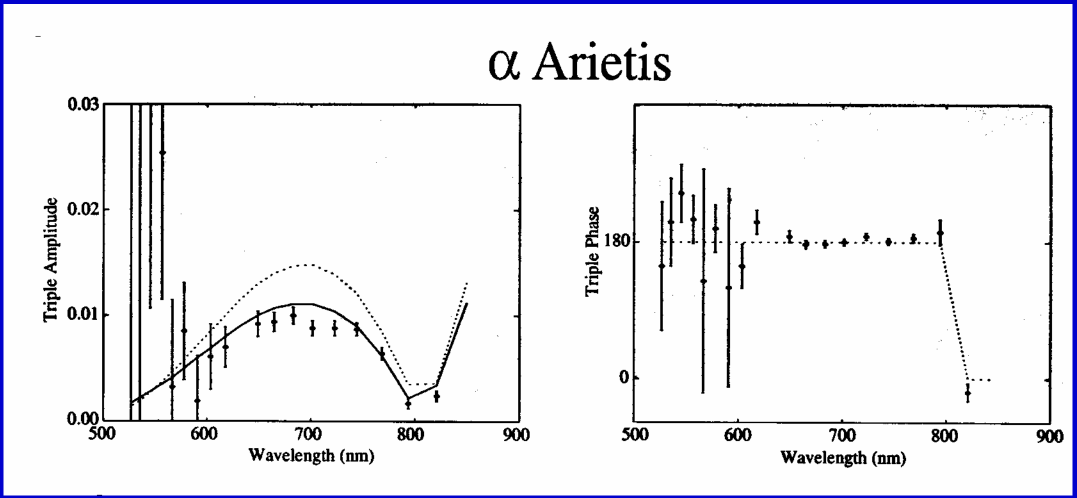

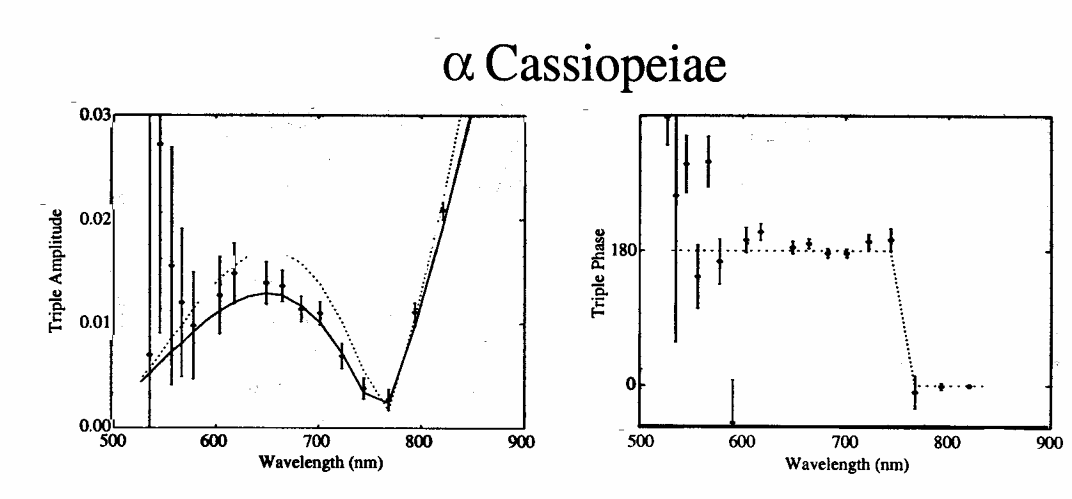

Triple Amplitude Closure Phase

Limb Darkening in Absorption Lines

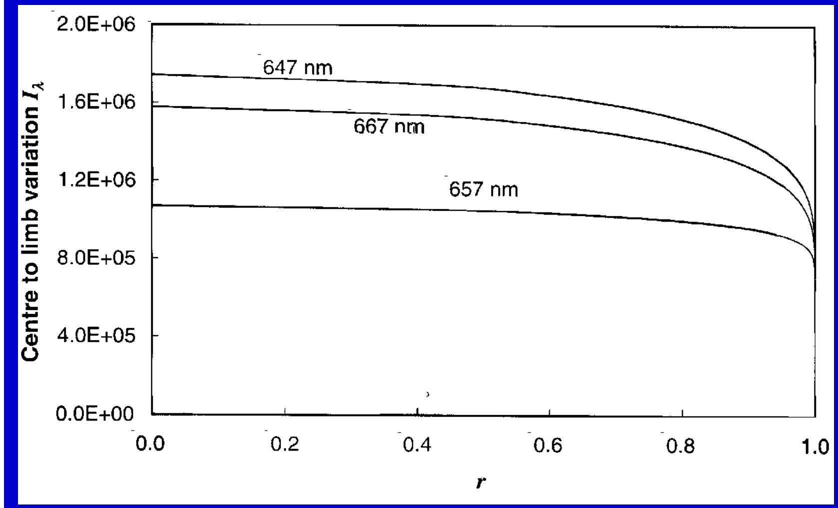

(Ref: Tango & Davis, MNRAS, 333, 642, 2002 – based on Kurucz model atmospheres)

Centre-to-Limb variation for Hα and adjacent continuum for an A0V star

(T_e = 10,000 K, log g = 4.0)

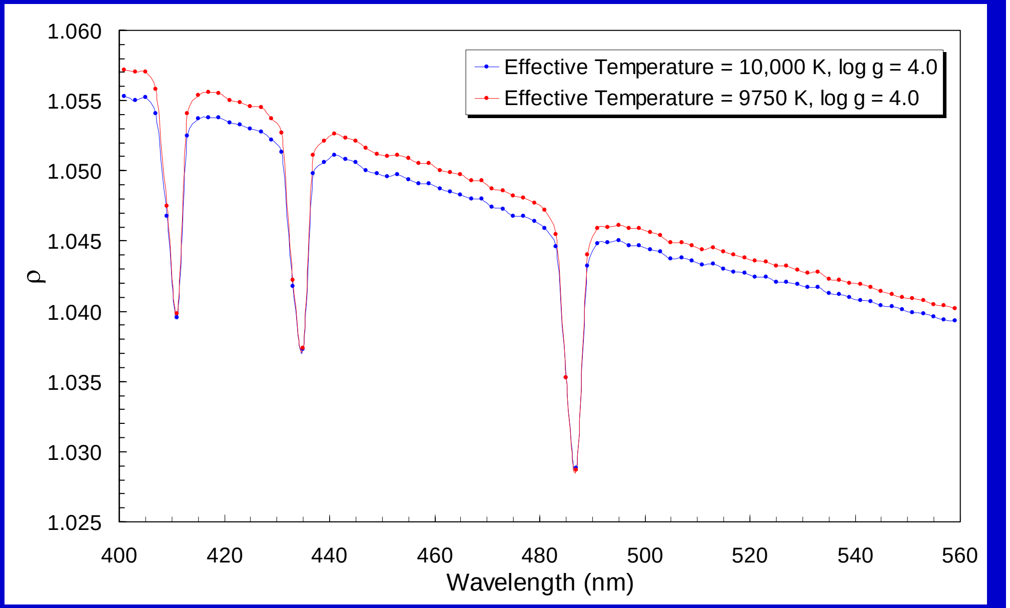

$\rho = \theta_{LD}/\theta_{UD}$ for Hβ, Hγ and Hδ

Rapidly Rotating Stars

Rapidly Rotating Stars

- Rapidly rotating stars are deformed into an ellipsoidal shape
- Surface gravity and flux are lower at the equator – polar brightened
- The deformation and brightness distribution affect the transform observed with an interferometer in opposite senses

Rapidly Rotating Stars

The model used for this illustration was generated by P. Strittmatter for the Narrabri Stellar Intensity Interferometer Programme

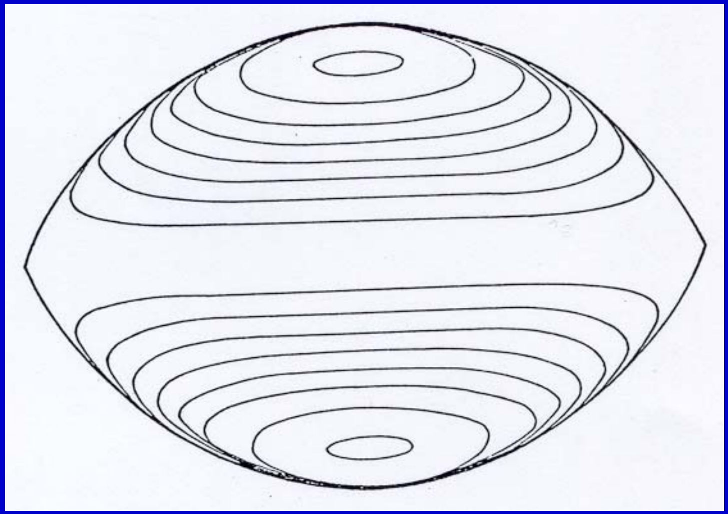

Projected brightness distribution for a star of spectral type A7 rotating at the critical velocity and seen equator-on at λ = 443 nm

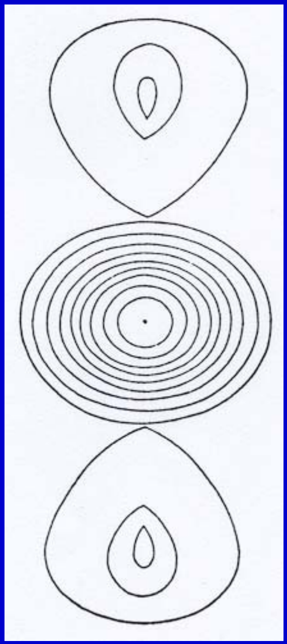

The central region of the (visibility)^2 function

Interferometric Responses

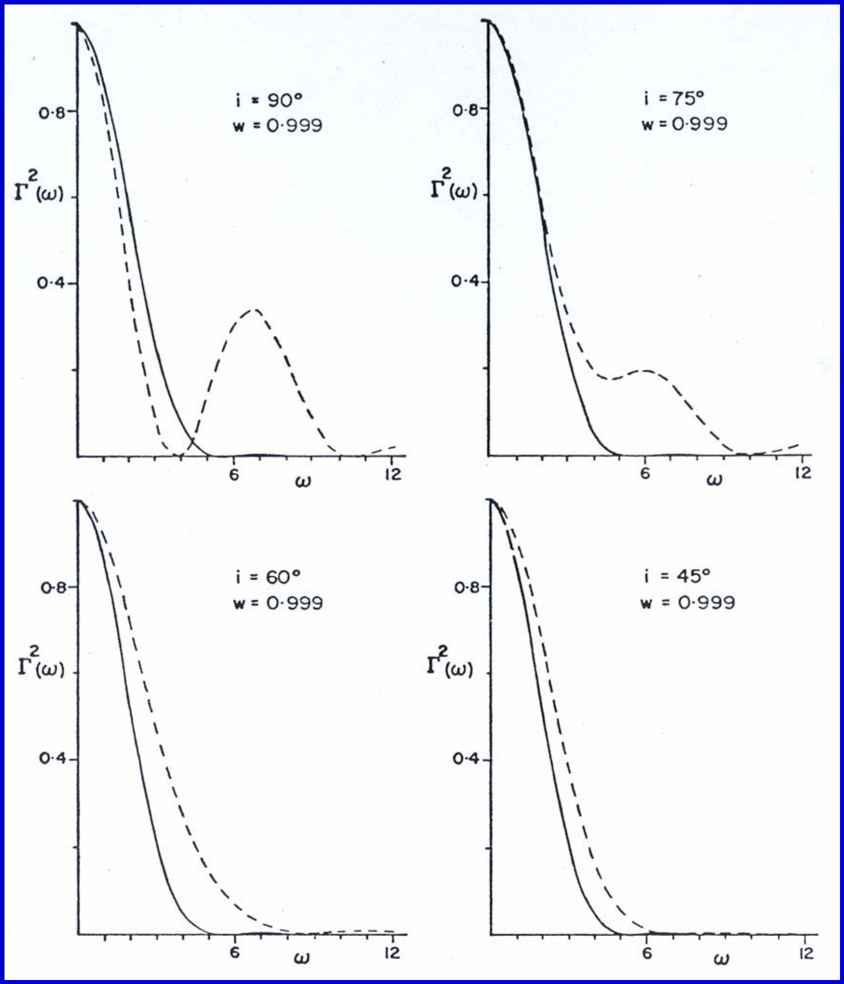

Cross-sections of the (visibility)^2 function for the axis of rotation at different inclination angles.

$\Gamma^2(\omega)$ = (visibility)^2

——— Cross-section perpendicular to the projected axis of rotation

- - - - - - Cross-section parallel to the projected axis of rotation

Altair (α Aql)

(van Belle et al., Ap.J.,559, 1155, 2001)

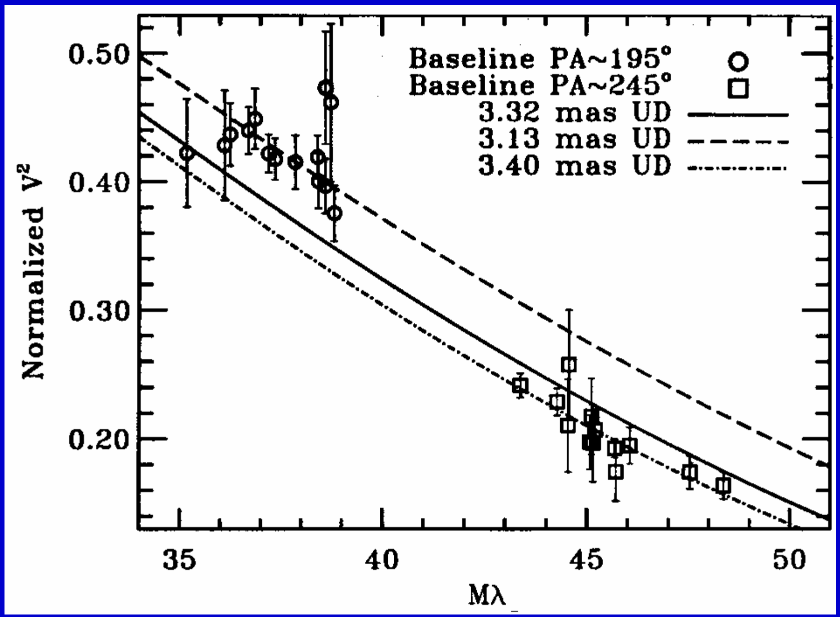

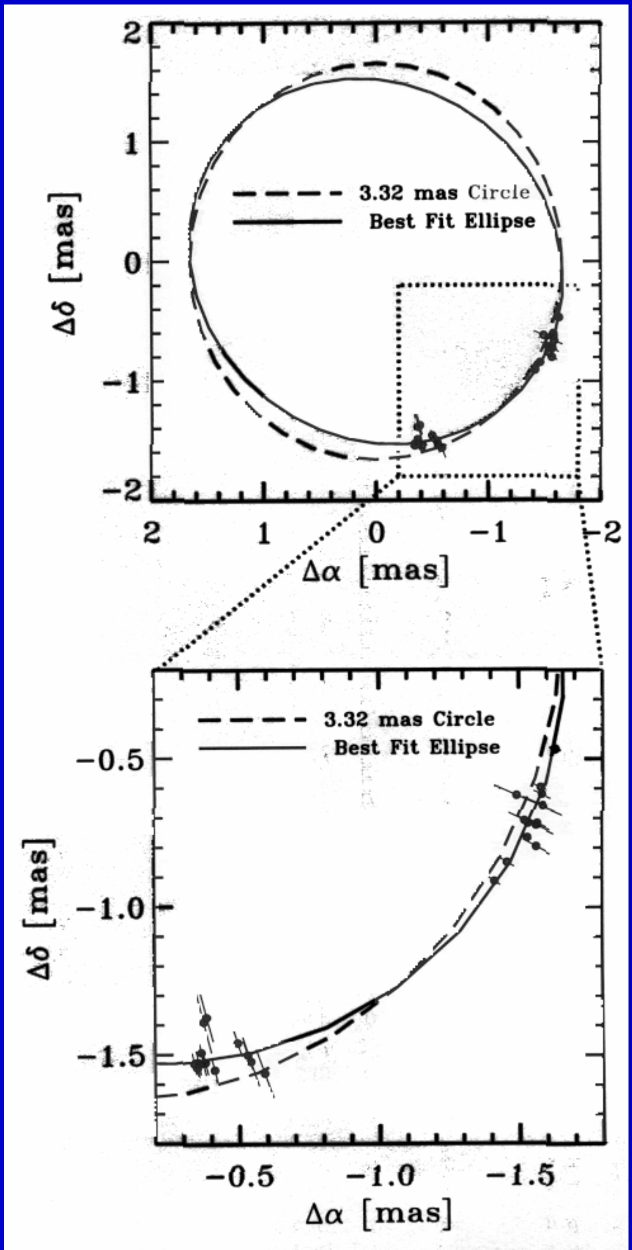

Visibility data

Best fit ellipse: a/b = 1.140±0.029

Altair (α Aql)

(From a Gerard van Belle slide)

- Diagrams show a fitted rigidly rotating Roche model
- Preliminary analysis indicates i ~ 45°, $v_{equator}$ ~ 300 km/s

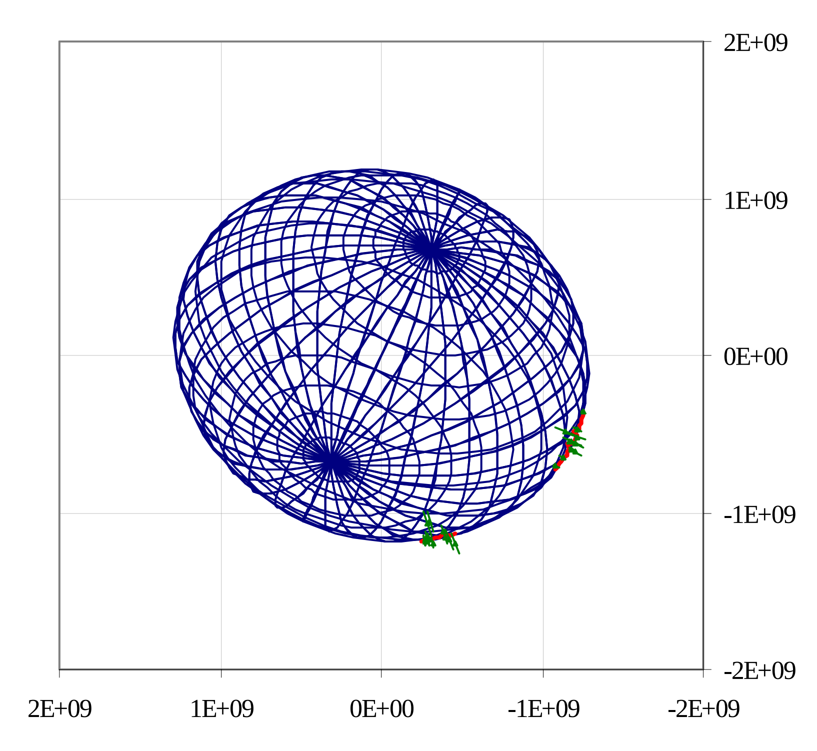

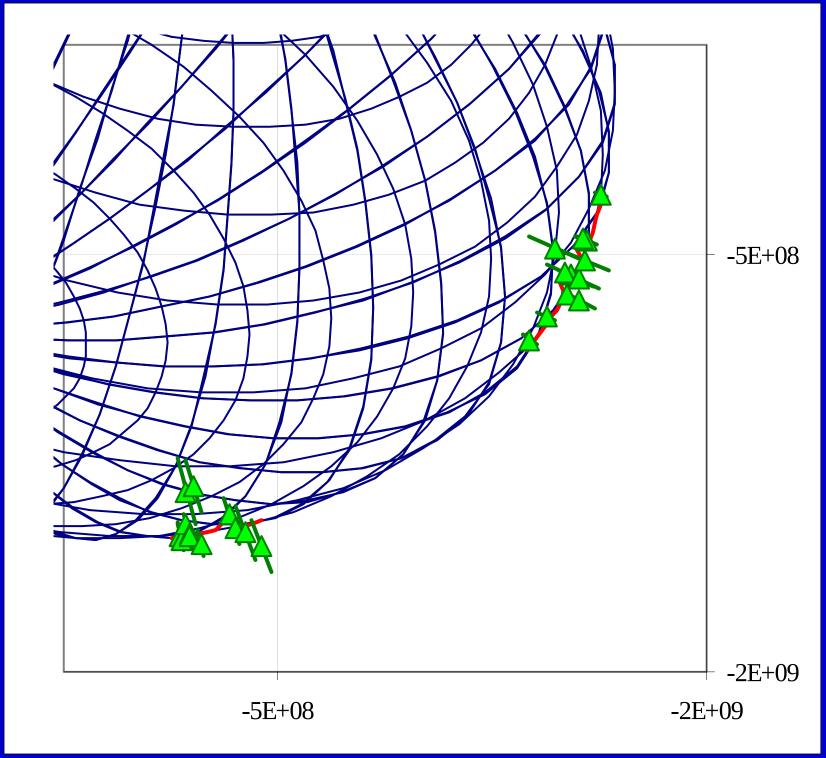

VLTI Observations of a Rapidly Rotating Star

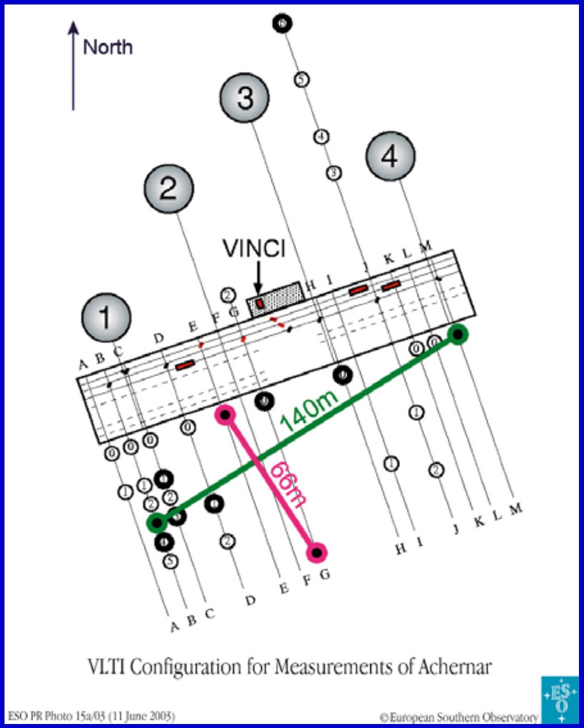

The baselines used

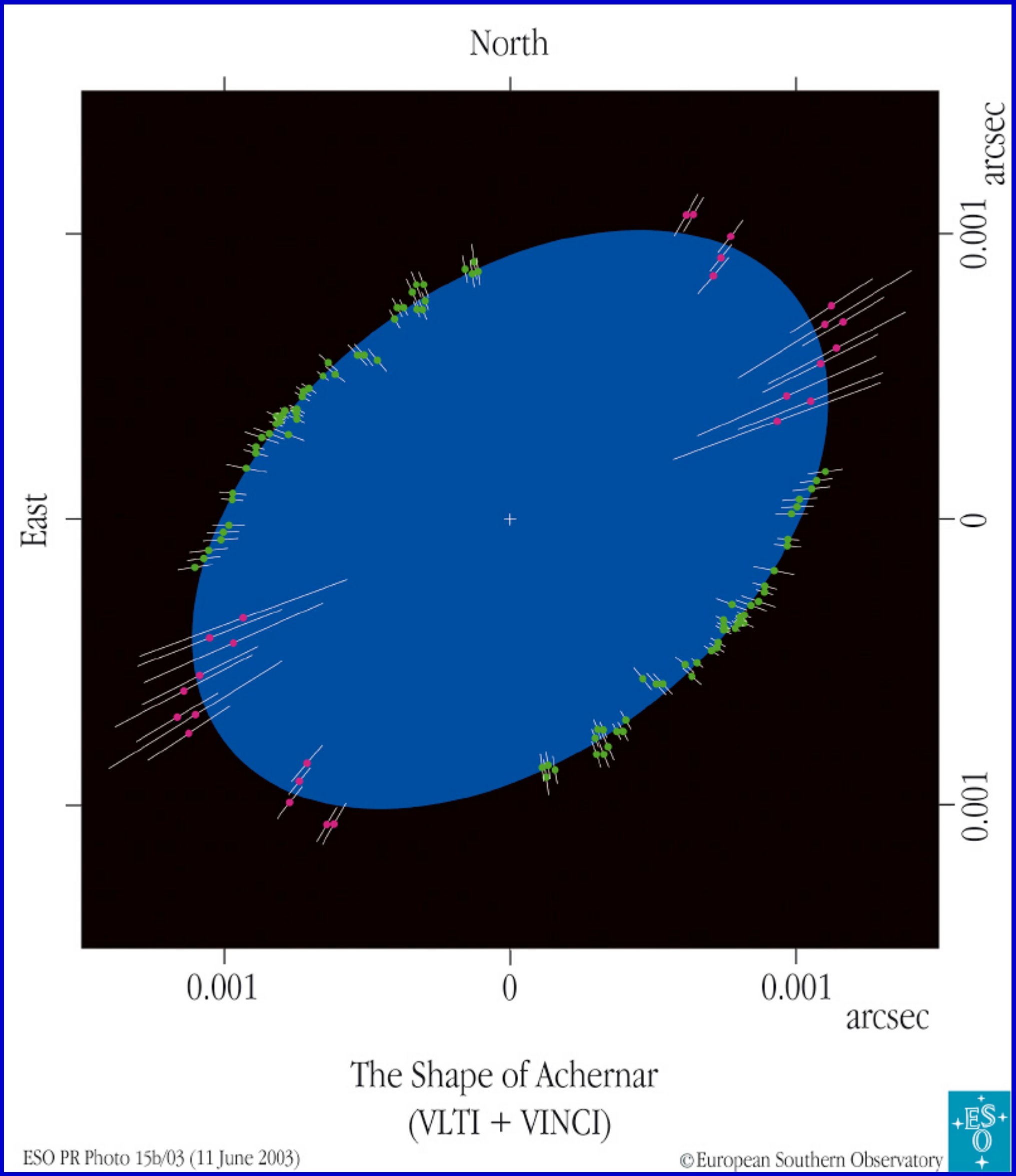

(Downloaded from the ESO Web Site)

Achernar (α Eri)

(Ref: Domiciano de Souza et al., astro-ph/0306277)

- Achernar is the brightest Be star in the sky
- Negligible emission during observations
- Uniform disk angular diameters: $\theta_{equ} = 2.53 \pm 0.06$ mas and $\theta_{pol} = 1.62 \pm 0.01$ mas
- Uniform disk diameter ratio: Equator/Pole = 1.56 ± 0.05

Limiting Models for Achernar

(Ref: Domiciano de Souza et al., astro-ph/0306277)

Fixed Parameters	Adopted Value	Comments
T_{pol}	20 000 K	~ B3V star
Mass	6.07 M_o	Harmanec (1988)
V_{equ}sin i	225 km/s	Slettebak (1982)
R_{equ}	12.0 R_o	
Model Dependent Parameters	Values for Model A	Values for Model B
T_{equ}	9500 K	14 800 K
i	50°	90°
V_{crit}	304 km/s	285 km/s
R_{pol}	8.3 R_o	9.5 R_o

Possible Limiting Models for Achernar (α Eri)

(Domiciano de Souza et al., astro-ph/0306277 & A&A, 393, 345, 2002)

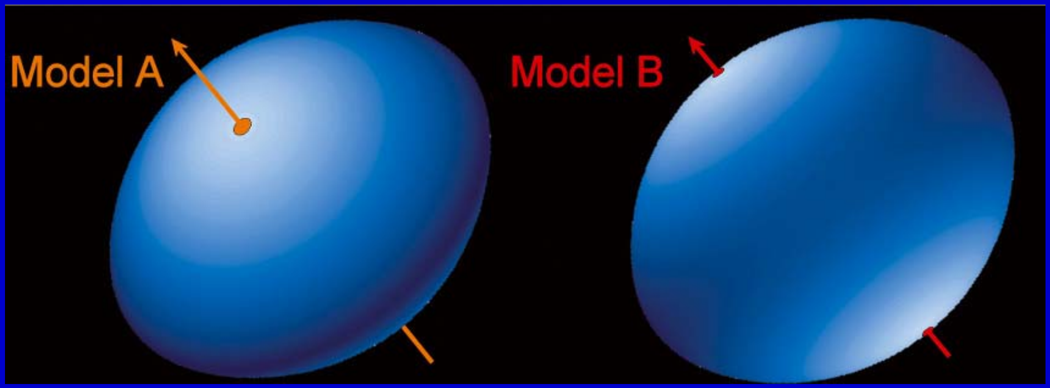

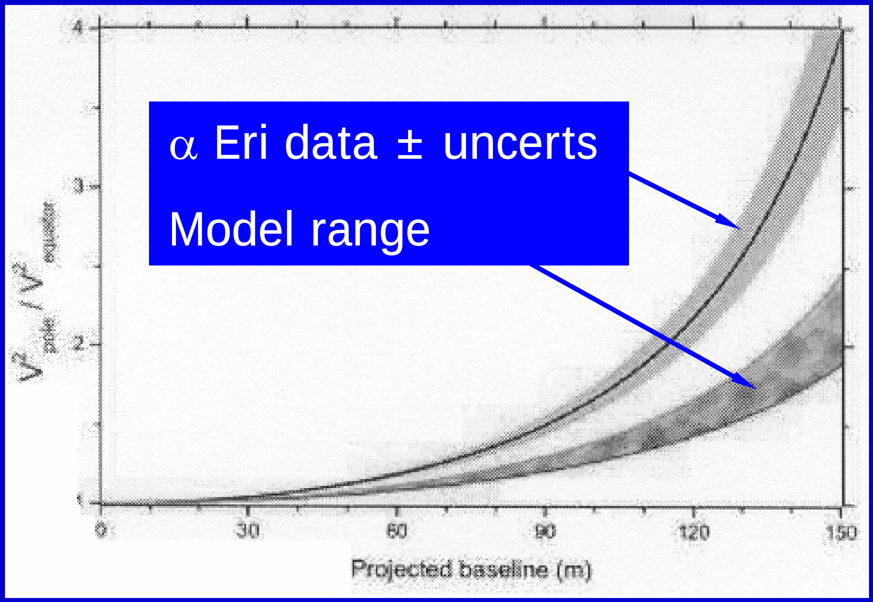

Achernar (α Eri)

(Ref: Domiciano de Souza et al., astro-ph/0306277)

- Conclude Roche approximation of uniform rotation and centrally condensed mass does not apply to Achernar

COAST Reconstructed Image of Be Star ζ Tau in Hα

(Ref: Young et al., SPIE 4838, 369, 2003)

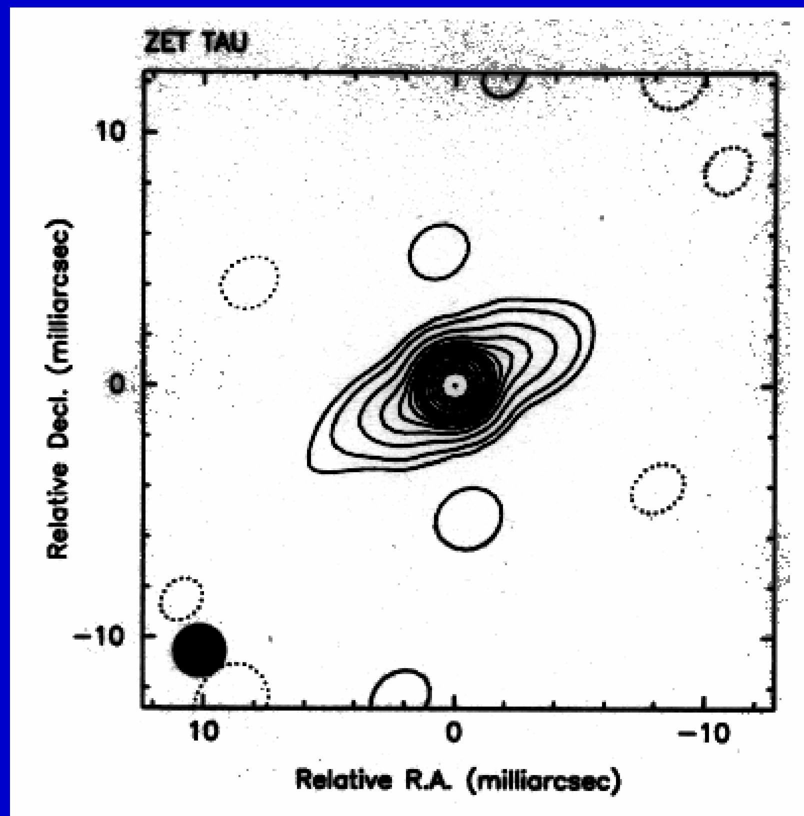

Image of the circumstellar envelope – the star is not resolved

Pulsating Stars

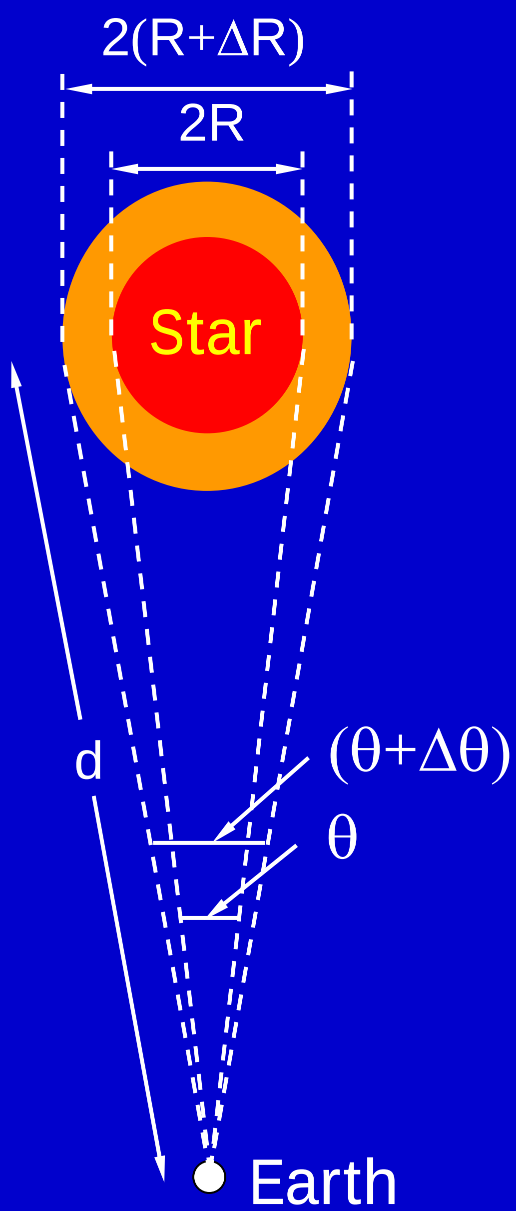

Pulsating Stars

Emergent flux $\mathcal{F}_\lambda$ and effective temperature T_e as for non-pulsating stars

Distance: $d = 2\,\Delta R/\Delta\theta$
(pulsation parallax)

With distance determined (or known) we can establish radius R and luminosity L

The Pulsation Parallax Method

- The combination of angular diameter measurements with linear diameter changes from spectroscopy to determine distances is known as the pulsation parallax method
- In the absence of direct measurements of angular diameters they have been derived from photometric surface brightness relationships (Barnes-Evans):

  e.g. $F_V = 4.2207 - 0.1V - 0.5 \log \theta$

  $F_V = a + b(V\text{-}R)$

- Relationships have been calibrated using angular diameter measurements of non-pulsating late-type giants and supergiants
- Given measured mean angular diameters of Cepheids the relationships can be calibrated directly with Cepheids

Cepheids – what has been achieved?

- Measurement of the mean diameters of several Cepheids by different interferometers
- Only two interferometric sets of measurements so far that convincingly show the angular pulsation

Mean Angular Diameters of Cepheids

The table lists only the latest published results for each interferometer

HR No.	Cepheid	Mean θ_{LD} (mas)	Instrument	Reference
8571	δ Cep*	1.60 ± 0.12	GI2T	A&A, 317, 789, 1997
		1.520 ± 0.014	NPOI	ApJ, 121, 476, 2001
2650	ζ Gem*	1.55 ± 0.09	NPOI	ApJ, 543, 972, 2000
		1.69 ± 0.16	IOTA	A&A, 367, 876, 2001
		1.675 ± 0.029	PTI	ApJ, 573, 330, 2002
7570	η Aql*	1.69 ± 0.04	NPOI	AJ, 121, 476, 2001
		1.793 ± 0.070	PTI	ApJ, 573, 330, 2002
424	α UMi	3.28 ± 0.02	NPOI	ApJ, 543, 972, 2000

* Used by Nordgren et al. to calibrate the Barnes-Evans relation (AJ, 123, 3380, 2002)

Measurements of Cepheid Angular Pulsations

ζ Gem was the first convincing measurement of pulsation

(Ref: Lane et al., Nature, 407, 485, 2000)

Cepheid	Mean θ_{UD} (mas)	Radius ($R_\odot$)	Distance (pc)	Instrument	Reference
ζ Gem	1.675 ± 0.029	66.7 ± 7.2	362 ± 38	PTI	ApJ, 573, 330, 2002
η Aql	1.793 ± 0.070	61.8 ± 7.6	320 ± 32	PTI	ApJ, 573, 330, 2002

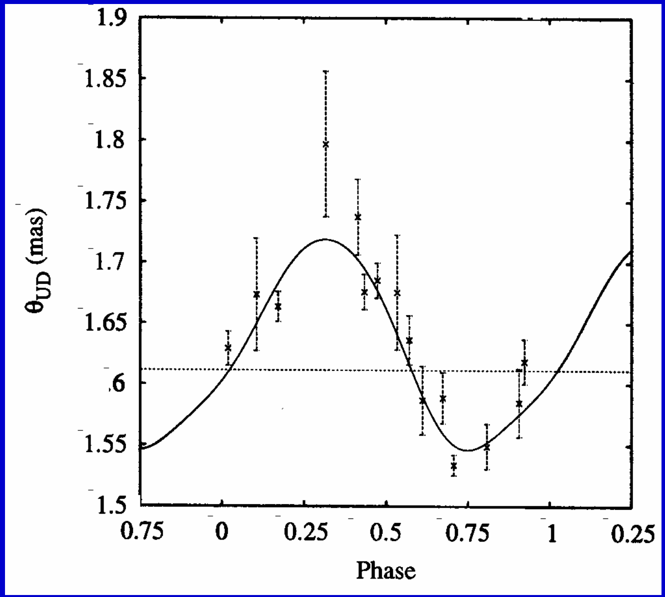

ζ Gem

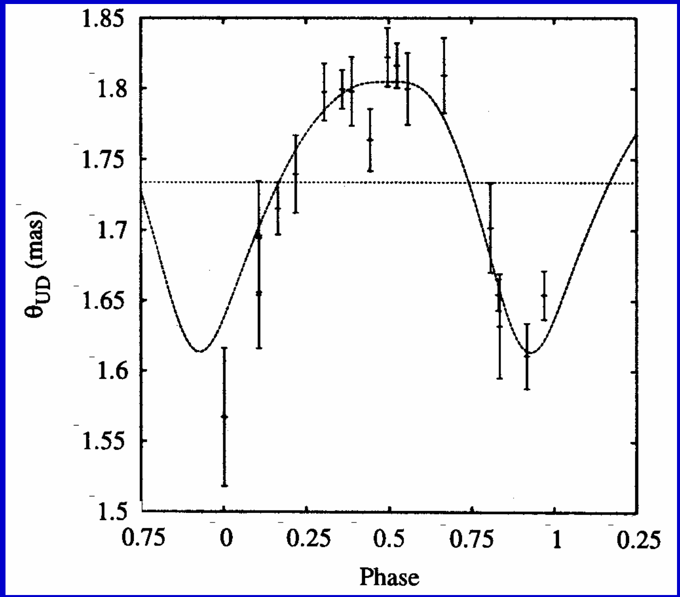

η Aql

The Distance to δ Cephei

(Ref: Nordgren & Lane, SPIE 4838, 243, 2003)

Distances via surface brightness relations

Source	Distance (pc)
HST parallax	278 ± 15
Mean(HST+H+A)	284 ± 14
F & G Non-Variables	259 ± 6
59 Cepheid measures	277 ± 9
η Aql (PTI)	279 ± 10
ζ Gem (PTI)	263 ± 6

Cepheids – Uncertain Factors and Conclusions

Uncertainties

- Pulsation factor – p-factor
- Radial velocity measurements – velocities depend on lines used, technique, velocity gradient in the atmosphere etc.
- Limb darkening
- Velocity differences in line and continuum forming regions

Conclusions

- ΔR will limit the accuracy of distance determinations
- Need hydrodynamic, non-LTE, pulsational models of Cepheid atmospheres to reproduce observed velocity curves, line asymmetries etc.
- Measurement of many Cepheids will improve accuracy and give an independent calibration of the zero point of the Cepheid luminosity scale

Miras - I

- Miras are long-period variables (150 < P < 500 days)
- These pulsating M giant stars have been observed with a number of interferometers
- The atmospheres are extended (not compact!)
- CLV shape may be strongly wavelength dependent and must be considered in obtaining meaningful diameters from fits to visibility data
- For example, strong TiO bands are formed substantially further out than the continuum

Miras - II

Variations in CLV shape transform to variations in the shape of the visibility v. baseline relationship

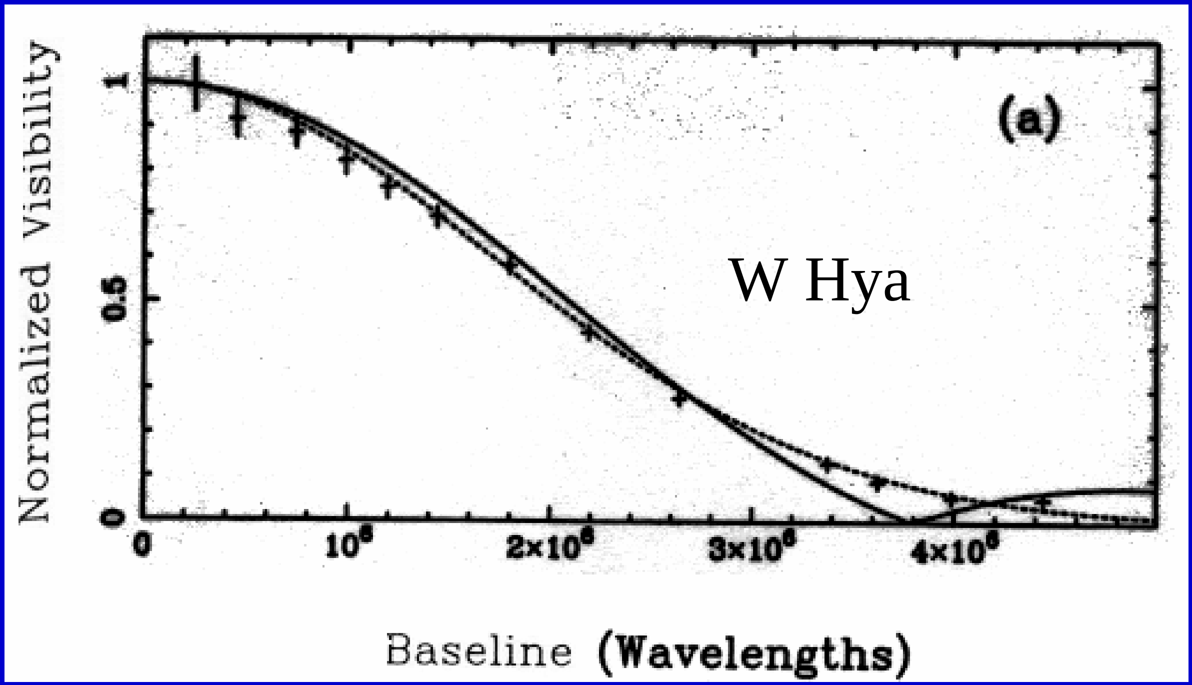

——— Model fit ----- Gaussian fit

(Ref: Haniff, Scholz & Tuthill, MNRAS, 276, 640, 1995)

Miras - III

- In the vicinity of molecular bands the angular diameter exhibits large variations

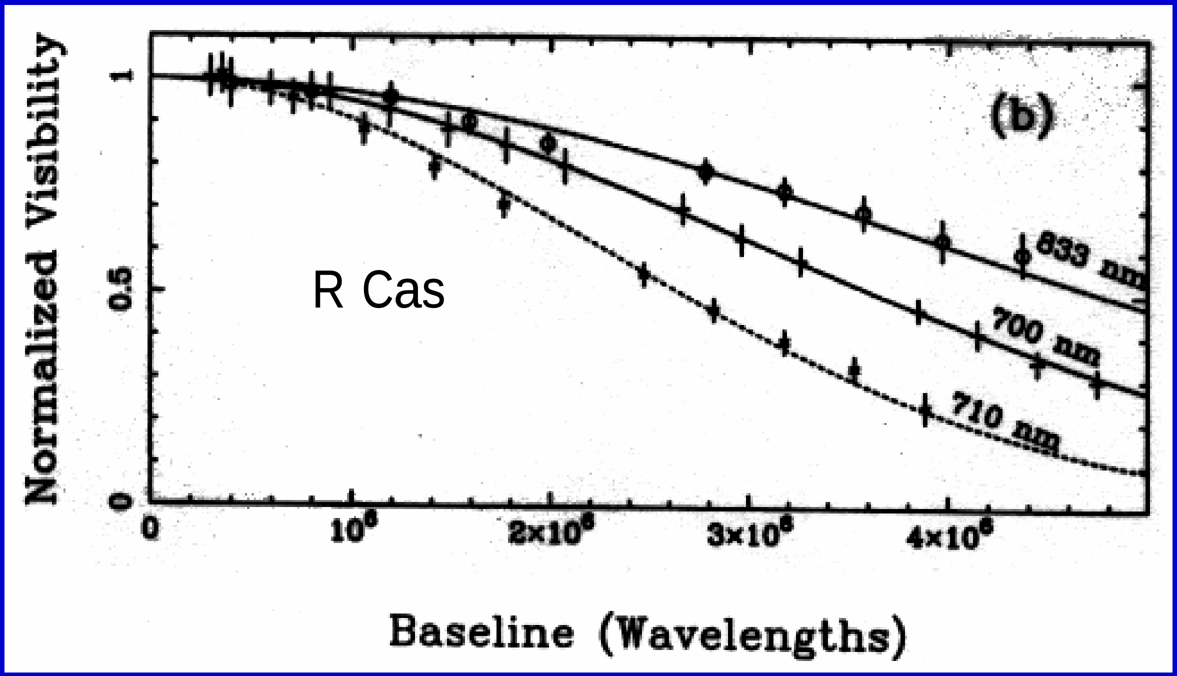

(Ref: Haniff, Scholz & Tuthill, MNRAS, 276, 640, 1995)

Diameter Changes of ο Cet Observed at 11 μm with the ISI

(Ref: Weiner, Hale & Townes, SPIE 4838, 172, 2003)

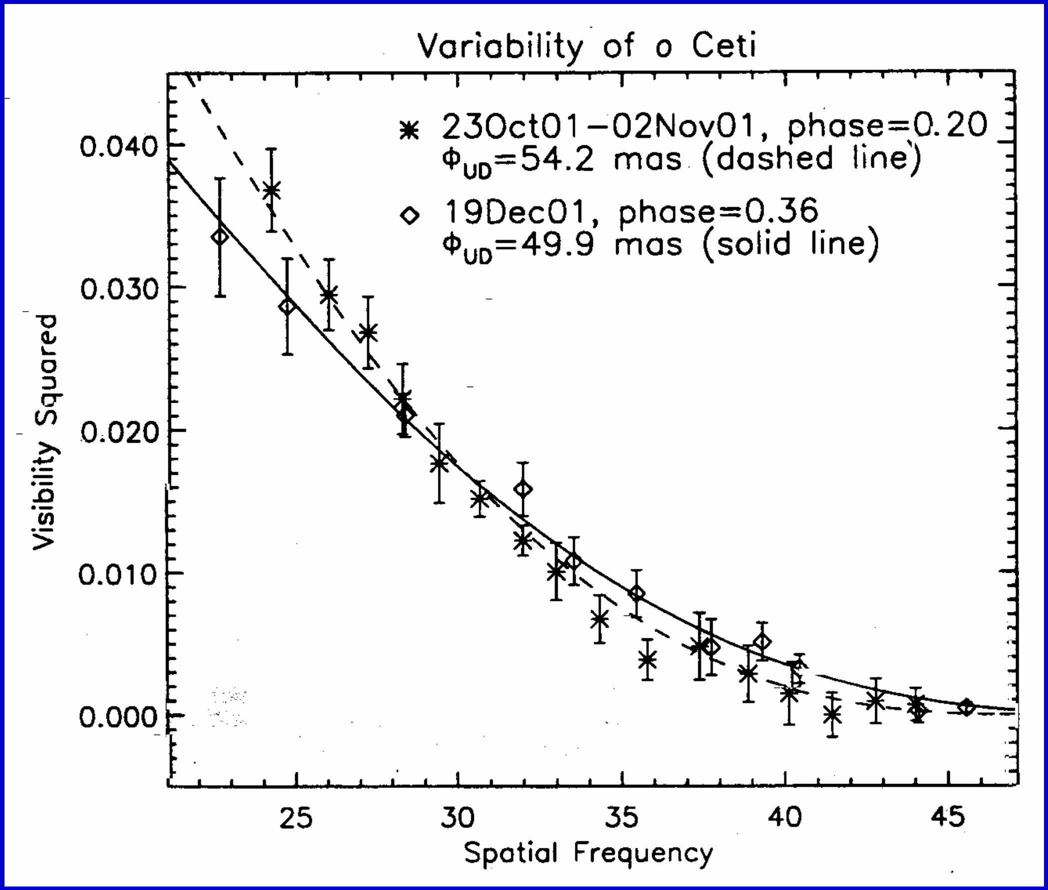

Best fit uniform disk curves at two different phases

Aperture Synthesis using IOTA & Keck Aperture Masking Data

(Ref: Monnier et al., SPIE 4838, 379, 2003)

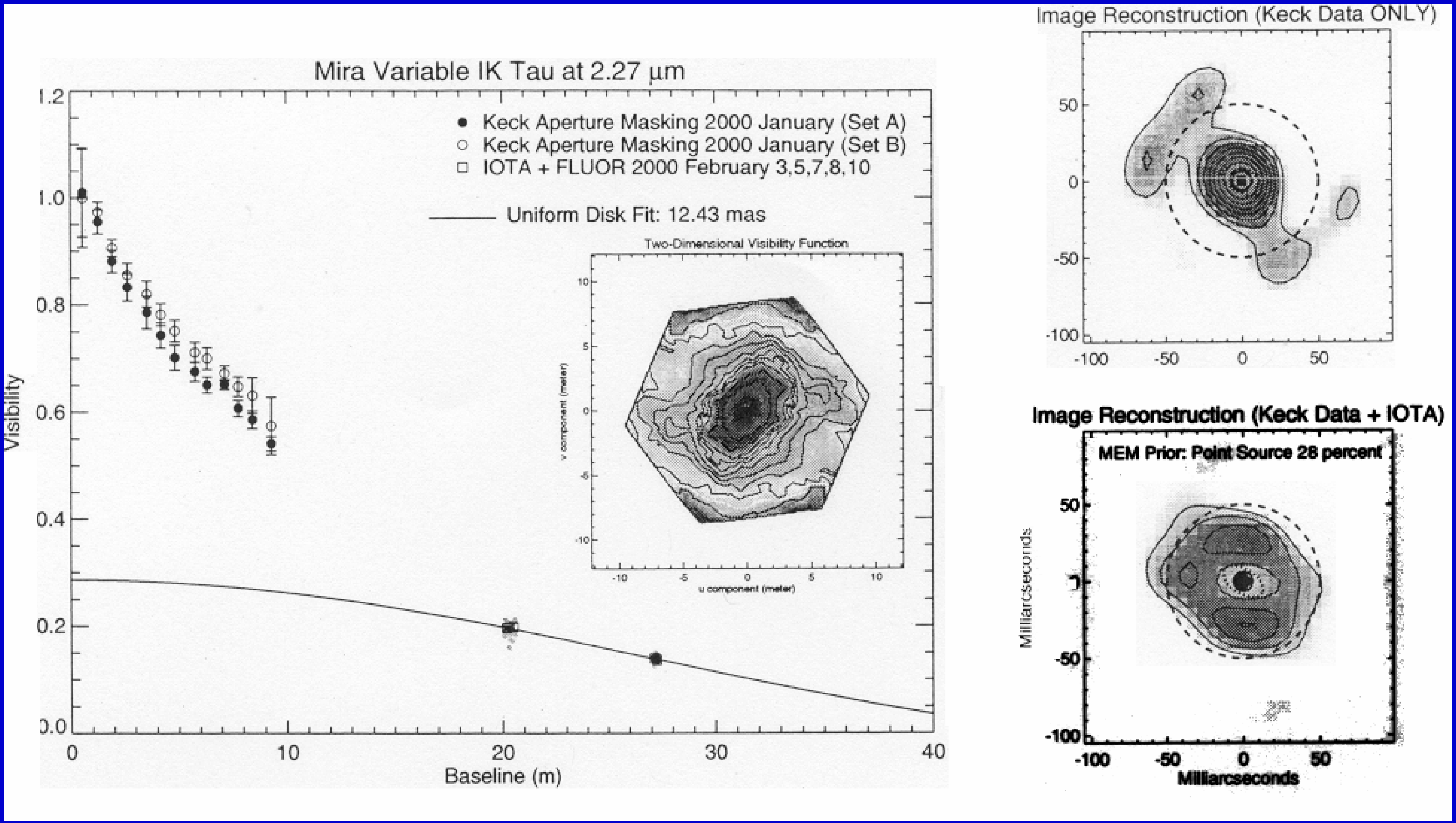

Miras

- Extensive observational programmes have been carried out with IOTA and PTI
- Paraphrased quotes from a recent paper from the PTI:
  - Wideband measurements of Miras can provide insight to basic parameters such as T_e and R
  - PTI measurements with 5 channels across the K-band (2.0-2.4 μm) can provide better insight to the chemistry and spatial extent of opacity sources than the full K band

(Ref: Thompson, Creech-Eakman and van Belle, SPIE 4838, 221, 2003)

Mira Quotes

Andreas Quirrenbach - "time series of measurements in well-defined narrowband filters covering several pulsation cycles will be required for a more detailed comparison between observations and theory . . .", not only with respect to limb-darkening and pulsation but also chemistry.

Michael Scholz - seeks (i) simultaneous observations with different baselines (to explore the shape of the CLV), (ii) simultaneous observations in different bandpasses (to probe atmospheric stratification), and (iii) observations in the same bandpasses at different phase-cycle combinations (to probe time variation of the atmospheric stratification)

Combining Results from Different Instruments

(Ref: Millan-Gabet et al., SPIE 4838, 202, 2003)

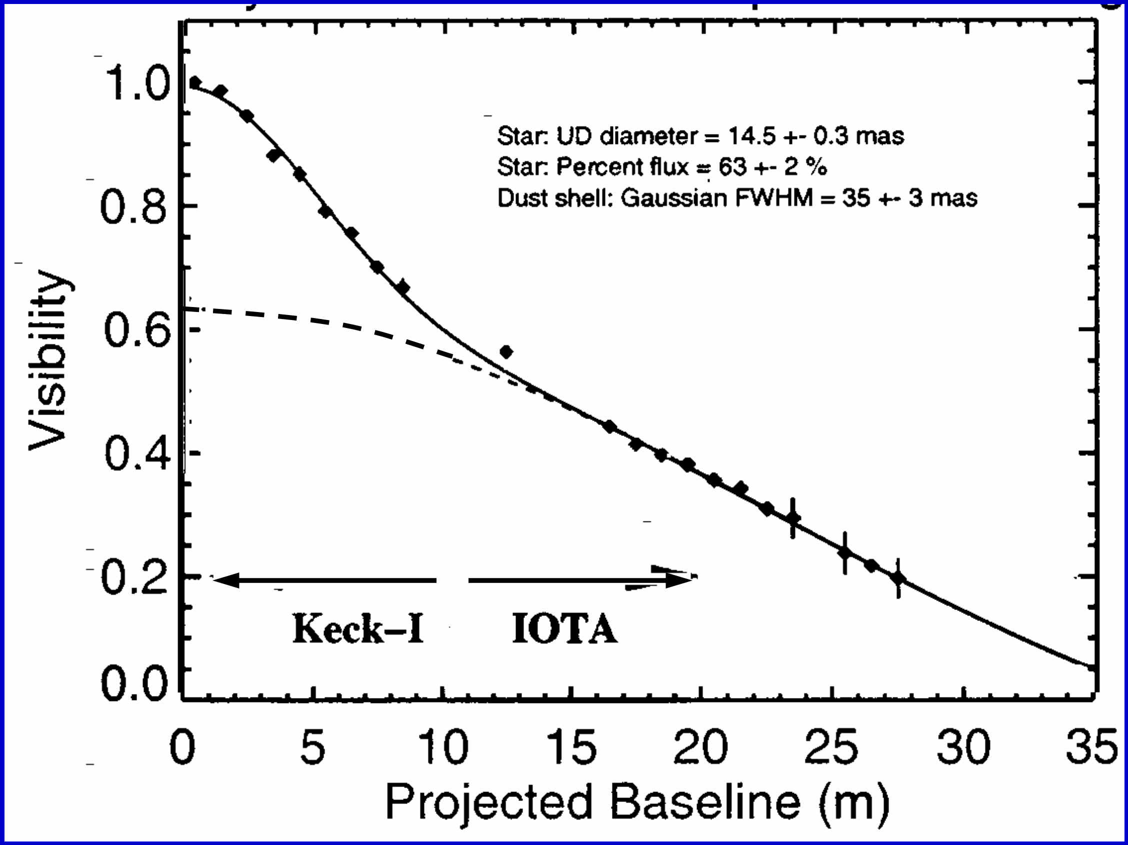

V Hya – IOTA and Keck Aperture Masking (K band)

Brightness Distributions for Betelgeuse

(Ref: Young et al., SPIE 4006, pp.472-480, 2000)

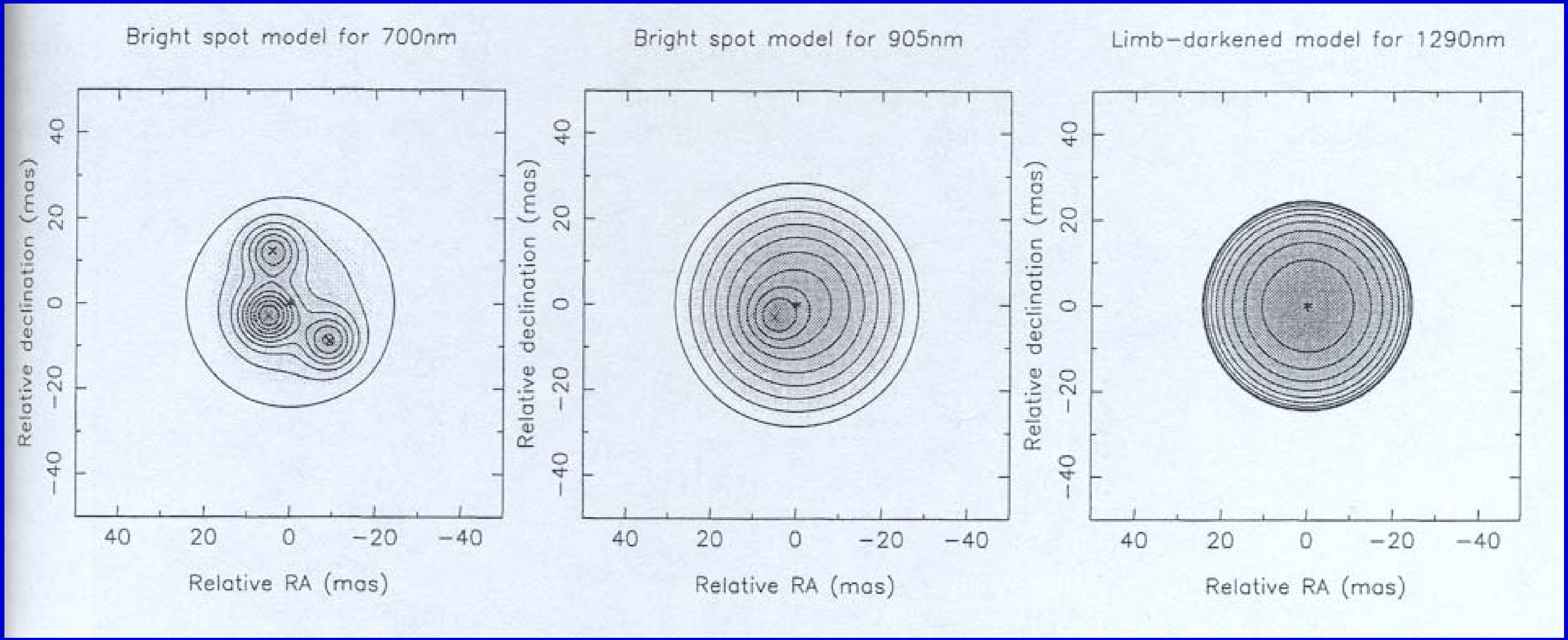

WHT COAST COAST

ISI 11 μm Angular Diameters for α Ori and o Cet

(Ref: Danchi et al., SPIE 4838, 33, 2003)

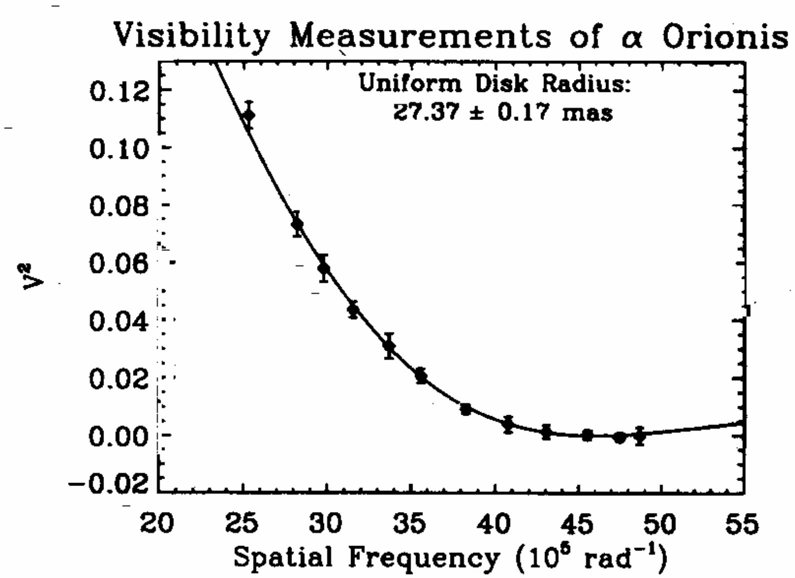

α Ori

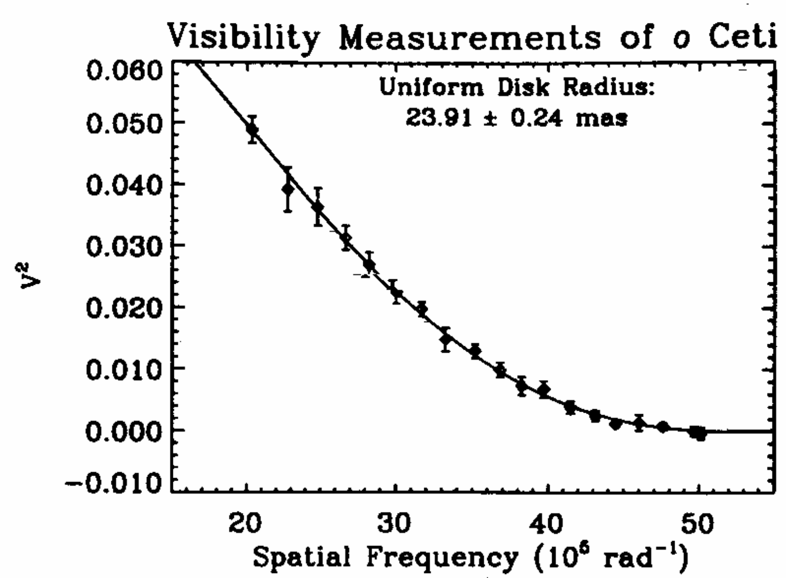

o Cet

Uncertainty in Effective Temperature

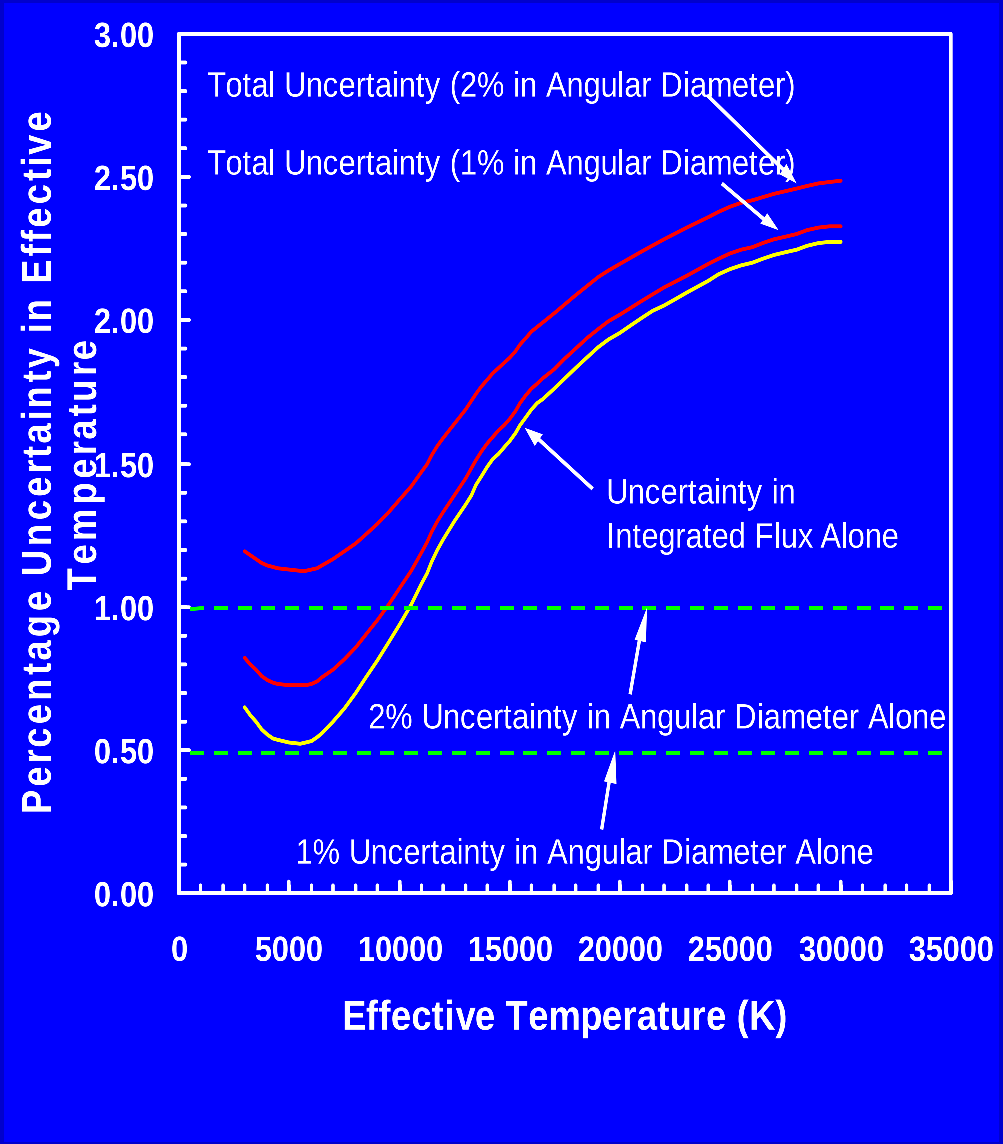

Complementary Data Required

(A)	For Effective Temperatures	Absolute flux distributions	Visual spectrophotometry Narrow band photometry UV and IR fluxes
		Limb darkening	Model atmospheres
(B)	For Radii and Luminosities	Distances	Astrometry (e.g. Hipparcos Data)
		Effective temperatures	From Item (A)
(C)	For Pulsating Star Distances, Effective Temperatures, Radii and Luminosities	Absolute flux distributions	As for Item (A)
		Change in radius	High resolution spectroscopy
		Limb darkening & separation of continuum and line forming regions	Model atmospheres